

***Petrodactyle wellnhoferi* gen. et sp. nov.:
A new and large ctenochasmatid pterosaur
from the Late Jurassic of Germany**

David W.E. Hone, René Lauer, Bruce Lauer, and Frederik Spindler

ABSTRACT

The Solnhofen archipelago of southern Germany has produced hundreds of fossils of pterosaurs in the last 250 years. In addition to recent descriptions and taxonomic revisions of existing specimens, new fossils continue to be uncovered and this includes important new material. In this paper we describe a mostly complete specimen of a ctenochasmatid pterosaur, which is one of the largest known pterosaurs from the Solnhofen area and one of the largest pterodactyloids in the Jurassic (wingspan estimated at c. 2.1 m). It also has one of the largest bony crests of any Jurassic pterosaur, and also has an unusual combination of short and spike-like teeth with an expanded frontoparietal crest that would have given it a strong bite despite the long and low skull. The nature of the specimen, mostly complete but almost entirely disarticulated, is unusual for the region. Despite well over two centuries of discovery, new pterosaurs continue to be discovered in these critical deposits that add to our knowledge of their diversity and ecology.

David W.E. Hone. School of Biological and Behavioural Sciences, Queen Mary University of London, Mile End Road, London, E1 4NS, UK. d.hone@qmul.ac.uk

René Lauer. Lauer Foundation for Paleontology, Science and Education, Wheaton, Illinois, USA. rene@lauerfoundationpse.org

Bruce Lauer. Lauer Foundation for Paleontology, Science and Education, Wheaton, Illinois, USA. bruce@lauerfoundationpse.org

Frederik Spindler. Dinosaurier Museum Altmühltal, Dinopark 1, 85095 Denkendorf, Germany. mail@frederik-spindler.de

Keywords: Pterodactyloidea; Mörnsheim; sexual selection; taphonomy; palaeoecology; new genus

Submission: 1 November 2022. Acceptance: 15 June 2023.

<https://zoobank.org/9EDC1671-0D3F-4125-AD7A-E299E1E4E1B8>

Final citation: Hone, David W.E., Lauer, René, Lauer, Bruce, and Spindler, Frederik. 2023. *Petrodactyle wellnhoferi* gen. et sp. nov.: A new and large ctenochasmatid pterosaur from the Late Jurassic of Germany. *Palaeontologia Electronica*, 26(2):a25.

<https://doi.org/10.26879/1251>

palaeo-electronica.org/content/2023/3878-a-new-solnhofen-pterosaur

Copyright: July 2023 Paleontological Society.

This is an open access article distributed under the terms of Attribution-NonCommercial-ShareAlike 4.0 International (CC BY-NC-SA 4.0), which permits users to copy and redistribute the material in any medium or format, provided it is not used for commercial purposes and the original author and source are credited, with indications if any changes are made.

creativecommons.org/licenses/by-nc-sa/4.0/

INTRODUCTION

The pterosaurs represent the first vertebrate clade to evolve powered flight (Witton, 2013) and although their fossil record remains fragmentary, a recent surge in research has led to a considerable increase in our understanding of their evolution, mechanics, ecology and diversity (Hone, 2012). In particular, the Late Jurassic (Kimmeridgian and Tithonian) limestone beds of the Solnhofen archipelago of Southern Germany have yielded huge numbers of well-preserved specimens of a wide variety of genera from multiple clades (Barrett et al., 2008).

The earliest pterosaur discoveries, dating back to the late eighteenth century, come from these beds (Ósi et al., 2010a), and there is a long history of research based around them. Despite this extended period of interest, the taxa from this region continue to undergo taxonomic revisions (e.g., Bennett, 1995, 1996, 2013a; Jouve, 2004; Vidovic and Martill, 2018). Furthermore, unappreciated specimens continue to be described from existing collections (e.g., Vullo et al., 2012; Hone et al., 2013), and some of these have been reinterpreted as new taxa (Vidovic and Martill, 2014), as well as the discovery of newly recovered material which can include new taxa (e.g., Frey et al., 2011; Hone et al., 2012a; Augustin et al., 2022; Martill et al., 2023).

Huge numbers of pterosaur specimens have been found in the region (e.g., Wellnhofer, 1970, 1975; Barrett et al., 2008; Hone et al., 2020) and while many are fragmentary and are preserved in near two dimensions, there are large numbers of complete and articulated specimens. A number of these show exceptional three-dimensional (3D) preservation and can include incredible and important details of soft tissues (Frey et al., 2003a). These fossil beds, therefore, provide important information on the evolution and diversity of pterosaurs since they include many of the last and largest of the non-pterodactyloid ‘rhamphorhynchoid’ pterosaurs (Woodward, 1902), early pterodactyloids (Witton, 2013), and most recently representatives of intermediate grade (or possibly clade), the non-pterodactyloid monofenestratans (Tischlinger and Frey, 2013). The most diverse group preserved in the Solnhofen area and associated beds are the ctenochasmatid pterodactyloids, a group of relatively long-legged animals that were primarily filter feeders (Martill et al., 2023) or predators of relatively small aquatic prey (Witton, 2013). Although the taxonomy of this group has been the subject of numerous revisions and repeated syn-

onymisation and splitting, there are certainly at least five genera present, and as many as eight have been recognised in one recent study (Vidovic and Martill, 2018).

Most Solnhofen archipelago pterosaurs are relatively small, partly through sampling which favours smaller (and younger) individuals (Bennett, 1995, 1996) but also because the apparent maximum sizes of these animals reached only around 2 m in wingspan (Elgin and Hone, 2020). Here we describe and identify a new ctenochasmatid pterosaur (Figure 1) based on a mostly complete specimen of a subadult animal, which shows a very prominent cranial crest and is among the largest known Jurassic pterodactyloids with an estimated wingspan of over 2 m.

Institutional Abbreviations

BSPG, Bavarian State Collection for Palaeontology and Geology, Munich, Germany; GPIT, Geologisch-Palaeontologisches Institut, Tübingen, Germany; LF, Lauer Foundation for Paleontology, Science and Education, Wheaton, Illinois, USA; MNHN, Museum National d'Histoire Naturelle, Paris, France; NHB, Naturhistorisches Museum Basel, Switzerland; NKMB, Naturkunde-Museum Bamberg, Germany; SMNS, Staatliches Museum für Naturkunde, Stuttgart, Germany.

METHODS

The specimen was prepared under microscopy using both pneumatic, and pin and needle tools. Binding agents of Starbond Super Thin Fast and Akemi 1000 were used to consolidate bones and matrix as appropriate.

The specimen was described primarily under visible light and when necessary, a hand lens. The specimen was illuminated with various UV lights during the description (e.g., see Figure 2). Additional observations were made from photographs under visible light and UV light as appropriate.

Ultraviolet Induced Fluorescence (UVIF) Digital Photography was used to document the specimen. UVIF photographic documentation was performed with the use of the following photographic equipment: Nikon D4 DSLR camera, and lenses: AF Nikkor 28 mm f2.8, AF-S micro Nikkor 60 mm 2.8G ED, and Nikkor 105 mm lens. Filters included: circular linear polarizing filter (used for all visible light and UVIF photography), MidOpt PRO 32-62; (+ polarizing film on the lamp for visible light images); and a color correction filter (for UVIF photography), MidOpt LAT20-62 (orange).



FIGURE 1. Photo of specimen LF 2809, a new large ctenochasmatid pterosaur. Scale bar is 10 cm.

Lamps - for visible light (daylight) photography: Fotodiox ring lights (color temperature of 5500k) with diffuser and polarizing film (used in combination with the circular linear polarizing lens filter to reduce unwanted glare and provide definition). Lamps - for UVIF photography included: Quad High-Performance UV Lamp, equipped with 95 watt bulbs in wavelengths UV A (320 – 400 nm), UV B (280 – 320 nm), and UV C (100 – 280 nm), with Hoya U-325 and Komodo UV-400 filters. The UV wavelength bulbs were directed onto the specimen individually, and/or all together at once, to identify specific UVIF responses; and Convoy S2+ 365 nm UV with LG LED flashlights were used for further examination. All images were captured in a

darkened room with the visible light or UV lamp as the sole light source.

SYSTEMATIC PALAEOLOGY

PTEROSAURIA Kaup, 1834

Pterodactyloidea Plieninger, 1901

Euctenochasmatia Unwin, 2003

?Gallodactylidae Fabre, 1976

Pterodactyle wellnhoferi gen. et sp. nov.

zoobank.org/F00E0CA2-3CC2-44DD-8A9F-E7793C76A016

zoobank.org/56C6CC35-859E-4D19-B61C-E8892F96AFC9

Diagnosis

Ctenochasmatid pterosaur with the following unique characteristics: elongate skull (over 2.8

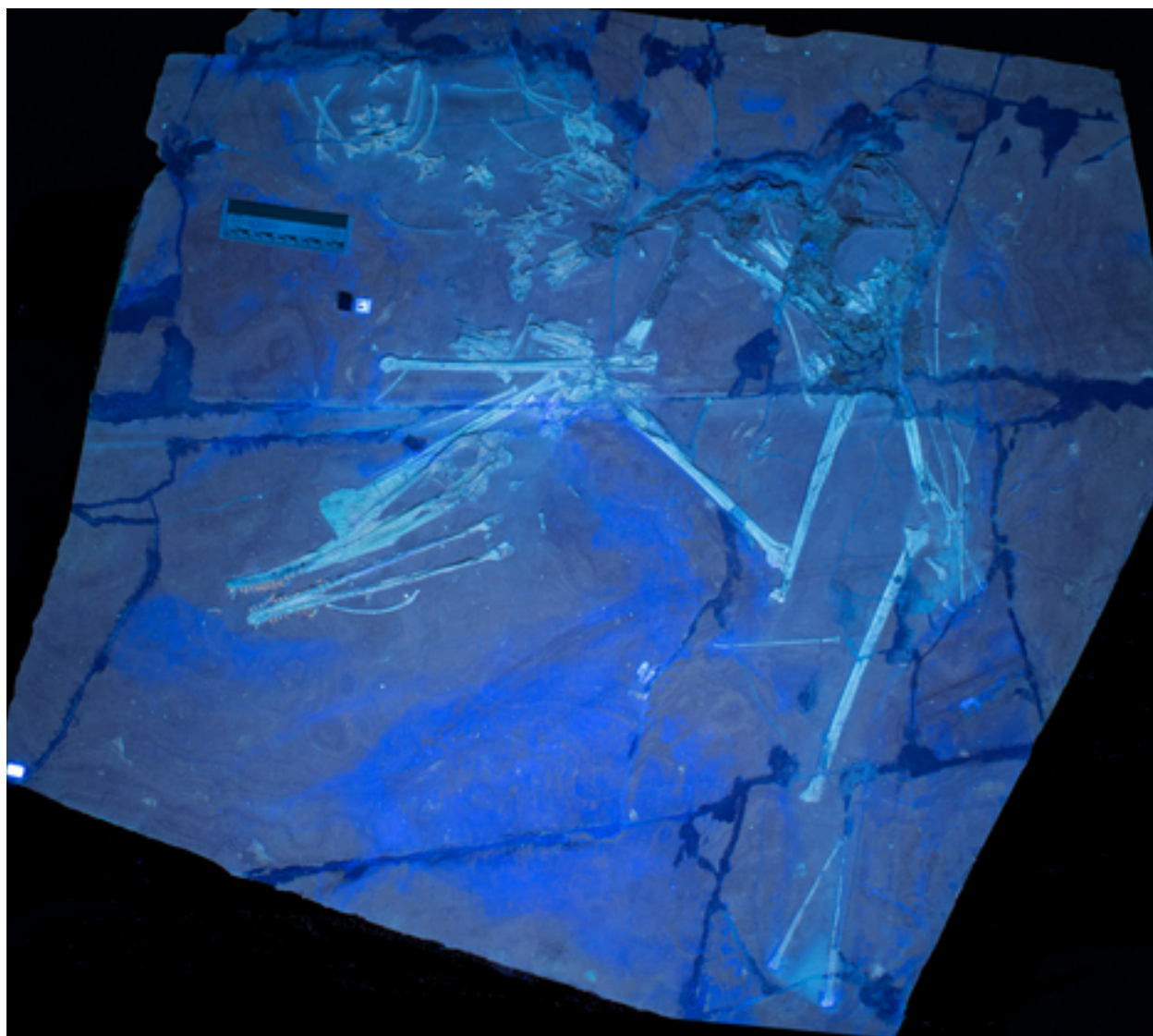


FIGURE 2. Photo of specimen LF 2809, a new large ctenochasmatid pterosaur under a mixture of UV A, B and C lighting. Scale bar is 10 cm.

times the length of the humerus); small frontoparietal crest; tooth spacing slowly increases along tooth row; either 23 or 24 teeth in each side of each jaw; elongate tibia (approximately 1.7 times the length of the femur).

Holotype

Specimen LF 2809 - an incomplete subadult individual consisting of the cranium and mandible, seven cervical and 12 dorsal vertebrae, shoulder girdles, a partial pelvis, numerous ribs and gastralia, both wings and one hindlimb.

Etymology

'*Petro*' from the Ancient Greek for 'stone' and '*dactyle*' from *dactylus*, for finger. This name harks

back to the original description of the first pterosaur, *Pterodactylus*, a ctenochasmatid from the Solnhofen archipelago which was called the 'Pterodactyle' at the time, however, the name 'Pterodactyle' appeared on the cover of the description (Cuvier, 1809), apparently in error. However, this name would have the appropriate etymology of 'stone-finger' and thus is echoed here. The species name '*wellnhoferi*' honours Dr Peter Wellnhofer who spent most of his career working on pterosaurs from the Solnhofen archipelago and associated beds.

Locality Information

The specimen was found in the summer of 2010 in the visitor's section of the Schaudiberg

Quarry near Mülheim, Bavaria, Germany. The Schaudiberg Quarry is located near the town of Mülheim which is part of the community of Mörnshheim/Gailachtal at the western end of the district of Eichstätt. This is in the region of Franconia between Nuremberg and Munich, in the state of Bavaria, Germany.

The specimen was found in the “Dritte Rosa Layer” (Third Pink layer) just below the Harte-Finze layer of the Mörnshheim Formation, Lower Tithonian, Jurassic and was collected at the following coordinates: 48.859 89° North, 10.99 267° East and with an elevation of 414 m. The Mörnshheim Formation is a series of laminated, lithographic limestones that are Lower Tithonian in age (Upper Jurassic) and is considered part of the Malm Zeta 2b-3 zone (Werner, 2005).

The specimen was found by an unknown collector and excavated by Ulrich Leonhardt and Roland Pöschl. It was prepared by Ulrich Leonhardt in April 2011 and was acquired by the Lauer Foundation in March 2015, and is permanently housed in the Lauer Foundation collection as LF 2809. A cast of the specimen was made by the Lauer Foundation, and donated to the Bayerische Staatssammlung für Paläontologie und Geologie, Munich, Germany, and is accessible there as SNSB-BSPG 2022 I 23.

Description

The specimen is preserved on a large (c. 80 cm wide and tall) and thick slab of lithographic limestone (Figure 1). The elements are mostly well-preserved and many are partially in three dimensions, although they are typically somewhat crushed. Some parts are very poorly preserved and are present as only an indistinct rough patch of bone and minerals. There are numerous associated bones present and most of the animal is represented. There is a largely well-preserved cranium in left lateral view, with the mandible presented in dorsal view. There are seven cervical vertebrae, 12 dorsal vertebrae, a partial sacrum and pelvic girdle, various ribs and gastralia, part of the shoulder girdle, nearly all elements of both wings, one leg and most of one foot (Figure 3). Only the sternum, the tail, and one leg are fully missing.

The specimen clearly represents an animal that is in an advanced ontogenetic state based on its large size, smooth bone texture, presence of an extensive cranial crest, complete fusion of the sacral vertebrae, the proximal and distal carpals into units, and complete fusion of the extensor ten-

don process on the first wing phalanx (Bennett, 1996, 2001). According to the growth indicators of pterosaurs by Kellner (2015), the fusion of the extensor tendon process would put this animal into category OS5 of pterosaur ontogeny, and the complete fusion of the epiphyseal plates of the humerus are among the last to fuse and have done so here which places this animal in category OS6 (the final one) and would be fully adult. However, Kellner (2015) notes also that for OS6, all bones and complexes are fused and that is not the case here. In LF 2809, the incomplete suturing of the cranial elements, and the incomplete obliteration of the fusion between the synsacral vertebrae to the sacrum (OS3-4) point to this animal not being fully mature. As a result, this animal appears to have not yet reached full osteological maturity, and it is perhaps best considered to be a subadult animal, although perhaps one close to full maturity. As it had not completely fused all of its elements at the time of death, it is likely that this animal was still growing and could potentially have been considerably larger at full size (Kellner, 2015). With an estimated wingspan of over 2 m at the time of death, this is a very sizeable pterodactyloid from the Solnhofen area.

Skull. The skull is well preserved overall and is in left lateral view, though the posterior part is less well preserved, and the skull has been obliquely crushed such that the palate and ventral part of the skull is visible (Figure 4). Several of the sutures between elements are visible as these have separated under compaction and so at least some of the individual pieces can be identified (Figure 5). In shape, the skull is long and low (258 mm long by 50 mm tall) and has a triangular profile. The naso-orbital fenestra (NAOF) is relatively small for a pterodactyloid (67 mm maximum length), and it is positioned in the back half of the skull (the anterior-most point is at the midpoint of the skull). The orbit is subcircular and large (26 mm wide by 25 mm tall). The upper temporal fenestra is small (c. 10 mm wide) though its shape is uncertain. The lower temporal fenestra is narrow and elongate (approximately 29 mm by up to 9 mm) and is inclined posteriorly.

The rostrum is slightly elevated giving the anterior snout an upturned appearance. This is similar to that seen in a number of ctenochasmatid species (e.g., *Ardeadactylus*, *Gnathosaurus*), although here the mandible (as seen) does not match this curvature (Figure 6A). This could be caused by the distortion to the cranium under crushing and torsion, or it could be the result of the

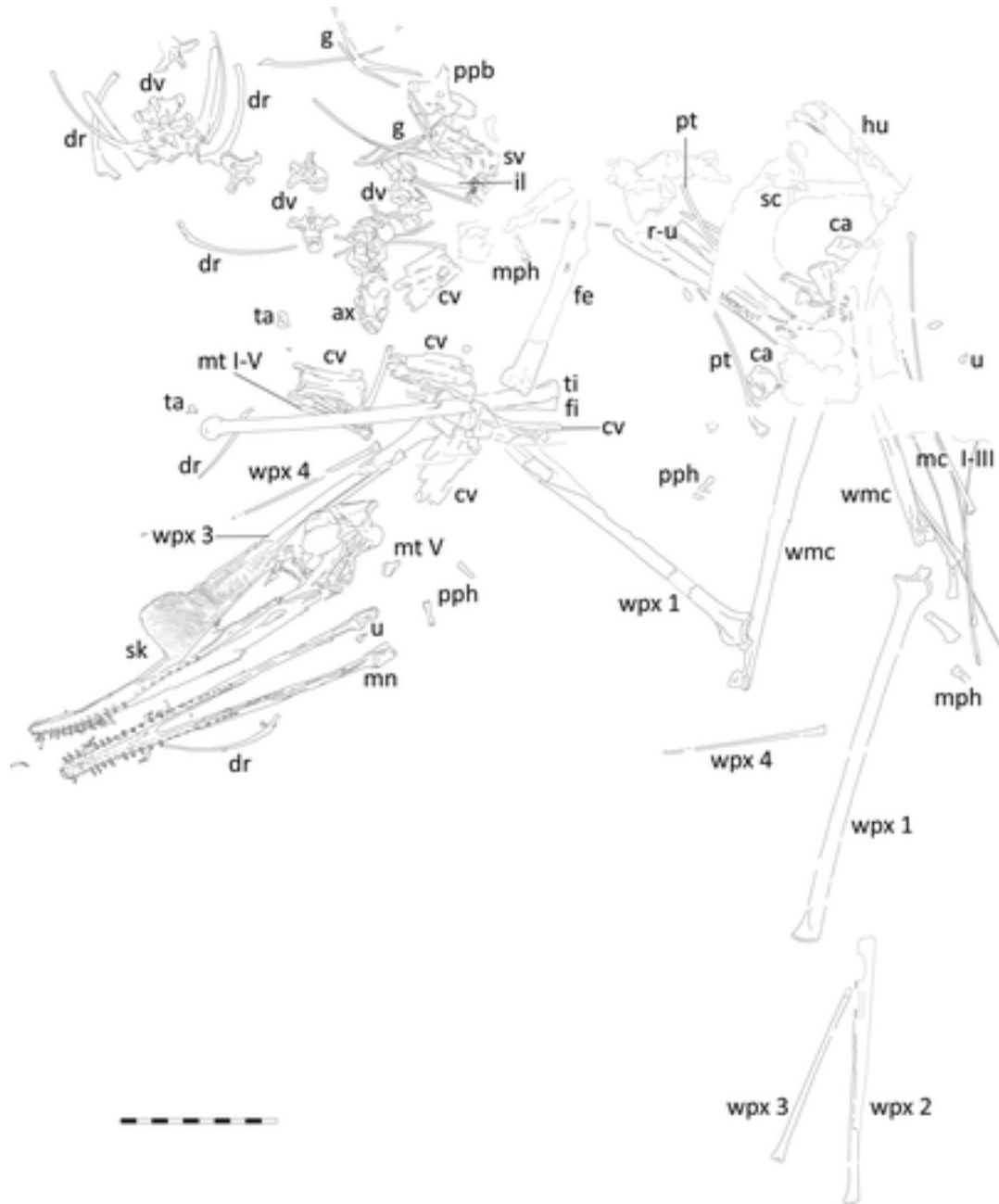


FIGURE 3. Tracing of specimen with labels. Abbreviations for this and subsequent figures are as follows: ax, axis; ca, carpal; cv, cervical vertebra; dr, dorsal ribs; dv, dorsal vertebra; fe, femur; fi, fibula; g, gastralia; hu, humerus; il, ilium; mc1-3, metacarpals 1-3; mph, manual phalanges; mn, mandible; mt I-V, metatarsals; ppb, prepubis; pph, pedal phalanges; pt, pteroid; r-u; radius and ulna; sc, scapulocoracoid; sk skull; sv, sacral vertebrae; ta, tarsal; ti, tibia; u, ungual; wmc, wing metacarpal; wpx 1-4, wing phalanges. Scale bar is 100 mm.

compaction of the mandible (or, less likely than either, that the upper and lower jaws did not match in curvature). Given the prominence of jaw curvature in ctenochasmatooids, and the lack of distortion to other parts of the skull (beyond some crushing), the curvature is considered likely to be mostly genuine. The suture between the premaxilla and max-

illa cannot be determined in the anterior part of the skull, but posteriorly as the maxilla folds up under crushing, the suture becomes apparent.

There is a tall (up to 32 mm) and very extensive (104 mm long), striated and anteriorly swept bony premaxillary crest (Figure 6B). This is tallest at the anterior margin of the crest and at least 5

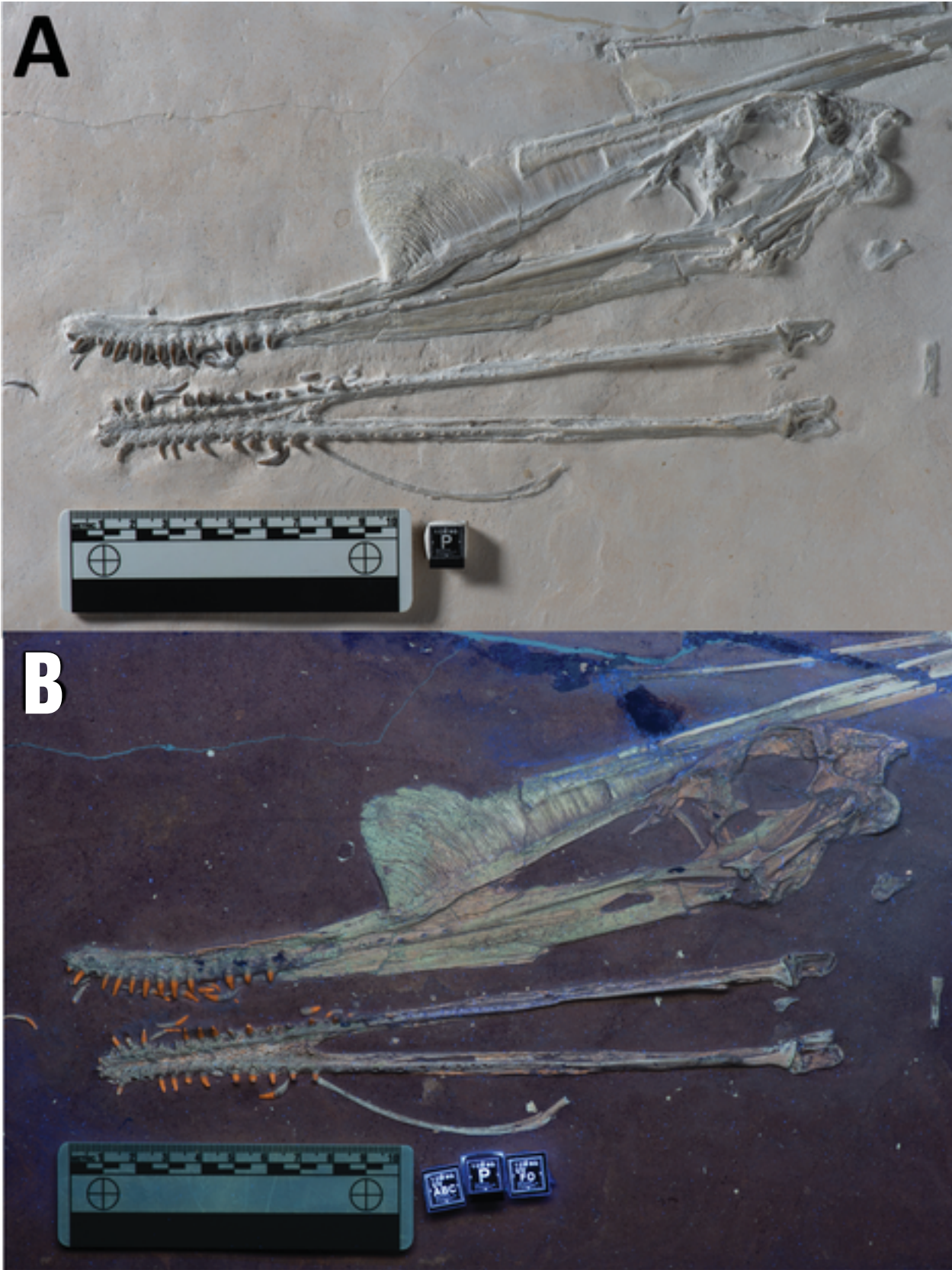


FIGURE 4. Close up of skull of *Petrodactyle* in A, natural light and B, UV light (mixture of UV A, B and C). Scale bar is 10 cm.

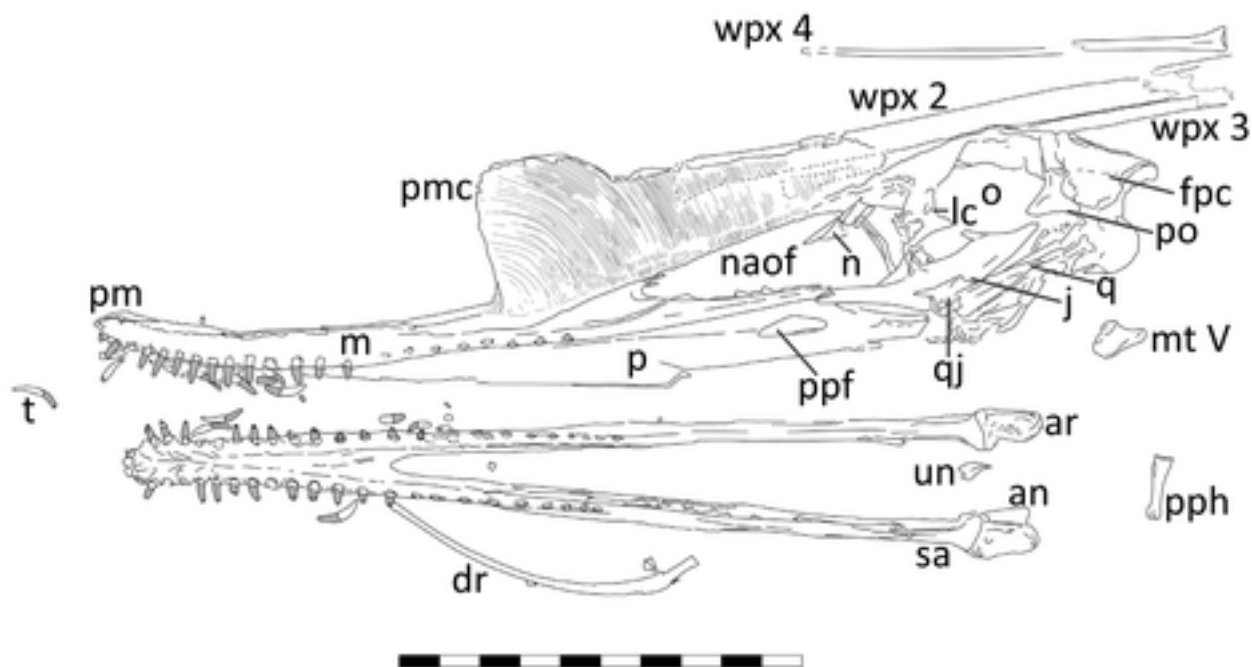


FIGURE 5. Tracing of the skull of *Petrodactyle*. Many sutures are uncertain and these labels are for general guidance. Abbreviations are as follows: an, angular; ar, articular; fpc, frontoparietal crest; j, jugal; lc, lacrimal; m, maxilla; n, nasal; naof, nasoantorbital fenestra; o, orbit; p, palate; po, postorbital; ppf, postpalatine fenestra; pm, premaxilla; pmc, premaxillary crest; q, quadrate; qj, quadratejugal; sa, surangular; t, tooth. Scale bar is 100 mm.

mm tall where it terminates, just in front of the lacrimal. The anteriodorsal part of the crest is notably less striated than the rest and has a different and apparently slightly more robust surface to it (this is most clearly seen under UV light combining A, B, and C wavelengths). The anterior most point of the crest has a noticeable depression where the grain of the bone tracks this (Figure 6C) and so it appears to be a quite natural furrow where the crest joins to the rostrum. This might represent some kind anchor for the soft tissue expansion which was surely present here as seen on many other pterosaurs with similar cranial crests (e.g., see Frey and Martill, 1998; Frey et al., 2003) (Figure 5).

The left nasal is an inverted 'L' shape with a short body making up the posteriodorsal corner of the NAOF and an elongate and thin process that extends into this fenestra. A second apparent projection anterior to this is the bar of the right nasal seen in medial view. Behind this is the robust and apparently distorted lacrimal. This is roughly triangular in shape and forms the anterior margin of the orbit and ventrally meets the jugal (Figure 5).

Posterior to the lacrimal is the frontal, which is large and makes up the dorsal part of the orbit and the skull roof. Posteriorly, the frontal has a ventral

projection, which meets and joins the postorbital, although the suture between the two cannot be determined. The postorbital is an L-shaped element and makes up the posterior part of the orbit, with the posterior ramus forming the ventral margin of the upper temporal fenestra and the dorsal margin of the lower temporal fenestra.

The parietal is integral with the frontal and forms the posterior most part of the cranium, and it sits behind the frontal and above the squamosal. This is a flat and subtriangular plate of bone that has a roughened texture and extends posterior to the occipital condyle as a projecting rear expansion to the skull as a frontoparietal crest.

The jugal is a very large triradiate bone making up a major part of the posteroventral skull. Its anterior ramus meets the posterior part of the maxilla and makes up the posteroventral part of the NAOF. The dorsal ramus meets the lacrimal and the posterior ramus meets the postorbital. It forms the ventral margin of the orbit and posteriorly the anterior margin of the lower temporal fenestra.

Behind the jugal is the quadratejugal, which in an elongate element that forms the posterior margin of the lower temporal fenestra. The quadrate cannot be identified. The right quadratejugal is present behind the left and is seen in medial view.

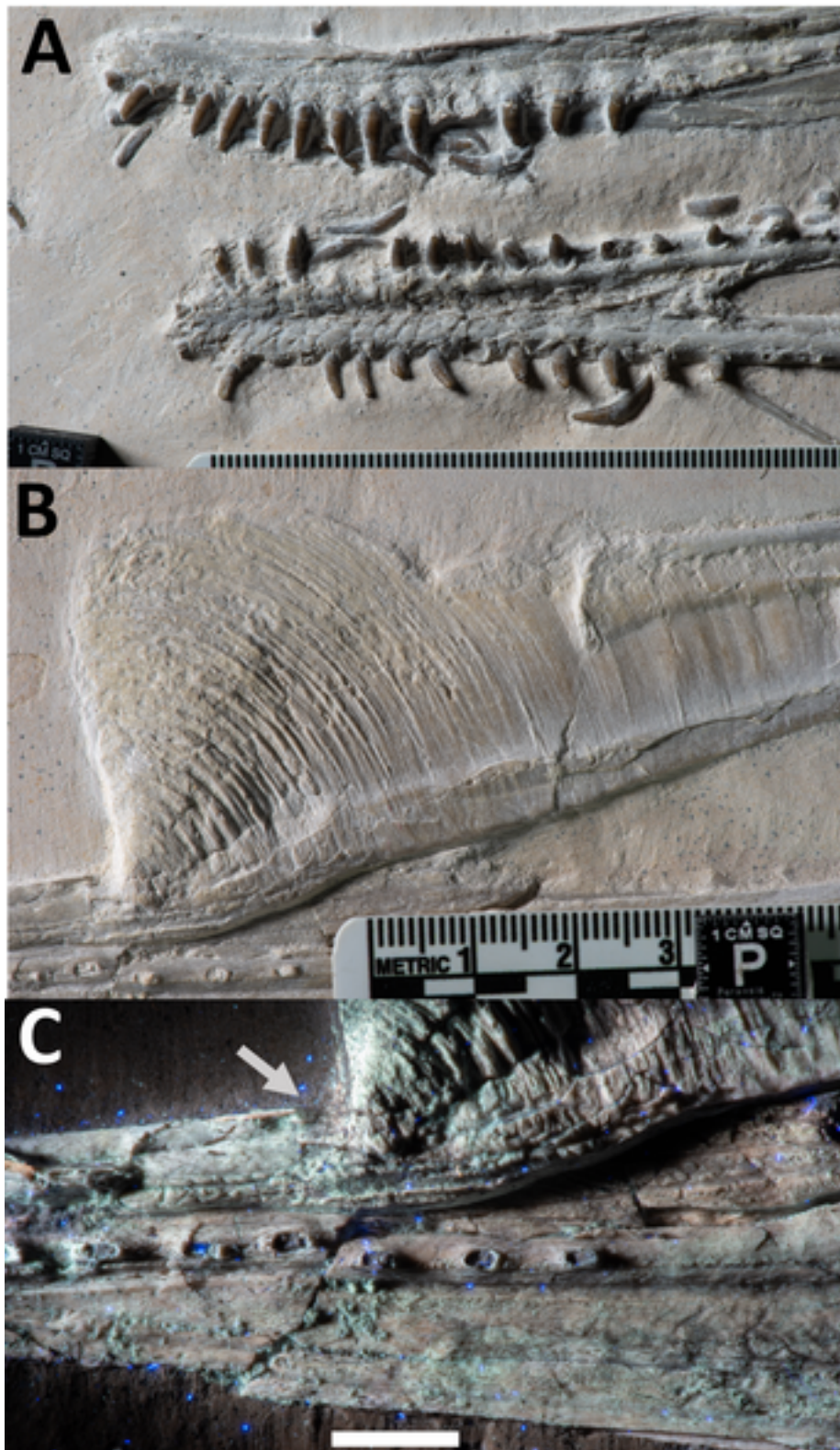


FIGURE 6. Close ups of key parts of the skull of *Petrodactyle*. A, detail of the upwards curved rostrum and anterior dentition under natural light (scale bar with 1 mm division). B, detail of the premaxillary crest under natural light showing the striations, the differing texture on the anteriodorsal part of this (scale bar in cm with mm divisions). C, photo of the notch at the anterior base of the crest (arrow), posterior alveoli and part of the palate under UV light showing (scale bar is 10 mm).

The quadrate is inclined at a strong angle, (approximately 30° from the horizontal) and dorsally this meets the squamosal which itself contacts the postorbital, but the sutures between these elements cannot be made out. Behind and posterior to the squamosal, the hemispherical occipital condyle is visible.

The oblique crushing of the skull has rotated the palate such that the left part of this is seen in ventral view (Figures 4, 6C). The palate of ctenochasmatooids may be solid for the anterior two-thirds of the skull, and even relatively robust posteriorly, as seen in *Gnathosaurus* (Ősi et al., 2010b, their figure 1E). Here, the palate was likely to have been somewhat convex, but crushing has folded this close to the midline such that the left side is partially visible. There is a subtriangular fenestra in the palate that is below the middle part of the NAOF and is considered here to be the postpalatine fenestra (Figure 5). Ventrally, there is a distinct notch in the displaced palate, and this is here interpreted as being the anterior margin of the subtemporal fenestra (sensu Ősi et al., 2010b) with the slight dorsoventral reduction in the height of the palate (as preserved) being the lateral margin of this opening.

There is a slight anterior expansion at the very tip of the jaw between the first pair of teeth, as seen in *Ardeadactylus* (Vidovic and Martill, 2018 supp. info.). The tooth row of *Petrodactyle* in the upper jaw is 118 mm long, measured along the curve of the upturned rostrum. There are a total of 23 teeth/alveoli in the upper jaw. The position of the final tooth is well anterior to the anterior margin of the NAOF. The teeth are generally evenly spaced, although the spacing gradually increases along the jawline, being approximately 2 mm apart in the front half of the tooth row and up to 5 mm apart in the posterior part. Unlike the mandible (see below) the first pair of teeth are not well separated from the rest of the tooth row.

The mandible is well preserved and presented in dorsal view to show its U-shaped profile (Figures 4, 6A). It has a maximum length of 227 mm and a maximum width of 37 mm and shows that the head was long and narrow. The symphysis is long and fully fused with no apparent suture visible between the two dentaries, and this is 68 mm in length along the midline. The transition from the dentaries into the surangulars are not visible. The posterior end of the surangulars expand slightly laterally and more so medially, and these are interpreted as enlarged points for attachment of jaw adductors.

Immediately posterior to the dentaries/surangulars sit the articulars (Figure 5). Each of these is a tongue-shaped posterior projection. On the left side of the mandible slight crushing has revealed the angular as a small piece of bone that lies slightly medial to the posterior part of the articular.

The splenial is plate-like and the left element is visible owing to its separation from the dentary. It is seen as a long sheet of medially positioned bone that reaches almost to the posterior end of the dentary. The two splenials appear to expand medially to form a shelf as seen in *Ardeadactylus* and *Cycnorhamphus* (Vidovic and Martill, 2018 supp).

A total of 23 teeth and/or alveoli are visible on the left side of the jaw and 24 on the right, with the posteriormost tooth of the right side being slightly posterior to that of the left (Figure 5). Measured along the dentary, the right side tooth line is 123 mm long and so slightly longer than the 118 mm of the left dentary row.

In the upper and lower jaws most of the anterior teeth are preserved but the posterior ones are missing, though the alveoli are clearly visible (Figure 6A, C). The teeth are mostly evenly spaced with 2 mm of space between each alveolus in the first half of the jaw, and in the posterior half of the tooth row this extends to approximately 4 mm. Notably however, there is nearly 5 mm between the first and second dentary tooth on each side such that the first pair of dentary teeth are slightly isolated from the rest of the row.

The hyoids are not preserved.

Dentition. The teeth are relatively small (the largest of the crowns are 5 mm tall), largely conical in shape and with slight medial curvature (Figure 6A). The roots are slightly longer than the crowns and taper to a point such that the isolated teeth on the slab have a banana-shape. The roots have fine grooves running along their length, though the enamel crowns are smooth and unornamented. The anteriormost teeth (the first five or so) are slightly smaller than the next 8-10 and after about the fourteenth tooth on each side these reduce in size (based on the size of the alveoli – Figure 6C). The tips of several teeth are worn, exposing the dentine and showing that the enamel is quite thick.

Cervical vertebrae. Seven cervical vertebrae are preserved (Figure 7) and collectively are seen in ventral, lateral, and dorsal views, making it difficult to determine the correct sequence of these, although the largest of these is cervical five. Mostly these are well preserved, though crushed, and one cervical is very poorly preserved and is left primarily as an impression with some bone fragments in



FIGURE 7. Close up of middle cervical vertebrae of *Petrodactyle*. A, in left lateral view, and B, in ventral view. Scale bar is 10 mm.

the matrix. The axis is crushed obliquely to primarily show the anterior and ventral face of the element and its form is difficult to make out. This is much shorter than the rest of the cervical elements and is not much longer than it is wide. It appears to have large and robust postzygapophyses that extend beyond the posterior margin of the centrum.

One has some slight damage to the ventral faces of a pre- and postzygapophysis, and it appears to be hollow inside suggesting these are highly pneumatic (see Figure 7B).

The following is a general description of the form of the non-axis cervical vertebra. The centra are rectangular in lateral view, being longer than

tall, and nearly rectangular in ventral view, being slightly wider than long, though with a slight constriction towards the middle part (Figure 7). The longest of these is very elongate and has a centrum length of 60 mm and is four times longer than tall. The prezygapophyses are robust and extend anteriorly in front of the flat anterior face of the centrum. As seen in ventral or dorsal view, the postzygapophyses are slightly larger than the prezygapophyses and do not extend beyond the posterior margin of the centrum. The neural spines are long, low, and blade-like and have a slight concavity towards their anterior margin (Figure 7A).

Dorsal vertebrae. Twelve dorsal vertebrae are preserved, and these are seen primarily in posterior view (Figure 8A), though several are crushed obliquely, and a series of three anterior dorsals are preserved in articulation and are seen in dorsal view (Figure 8B). In anterior and posterior views, the centra are nearly circular in outline with a slightly flattered dorsal margin and are mildly amphicoelous. The centra are short, being subequal in length, or slightly longer to their width. These have a clear midline constriction of centrum seen in both lateral and ventral view so that the centra are spindle-shaped.

The neural arches are tall being taller than the centra, although the neural spines are not very tall and typically only around half the height of the centra (Figure 8A). The pre- and postzygapophyses are small and rounded processes that extend slightly beyond the respective anterior and posterior margins of the centrum. The neural spines have a broad base and taper gently to a rounded tip in the posterior dorsals, but the anterior and middle dorsals have slight lateral expansions on their dorsal tips such that they are T-shaped in anterior view. The lateral processes are long, being around twice the length of the neural spine in the anterior dorsal vertebrae, and at least as long as this in the posteriormost dorsal vertebrae. In the anterior dorsal vertebrae, as seen in dorsal view, the lateral processes are broad and also have a notable anteroposteriorly expanded tip such that the process is also T-shaped. In anterior view, the lateral processes of the middle dorsal vertebrae have a slight but distinct posterior expansion to the middle part of the posterior margin of the process. These extensions are similar to those seen on the vertebrae of many extant birds where partially ossified tendons have fused to the vertebrae to help stabilise the joints (DWEH pers. obs.), there is, however, no indication that these anterior dorsal

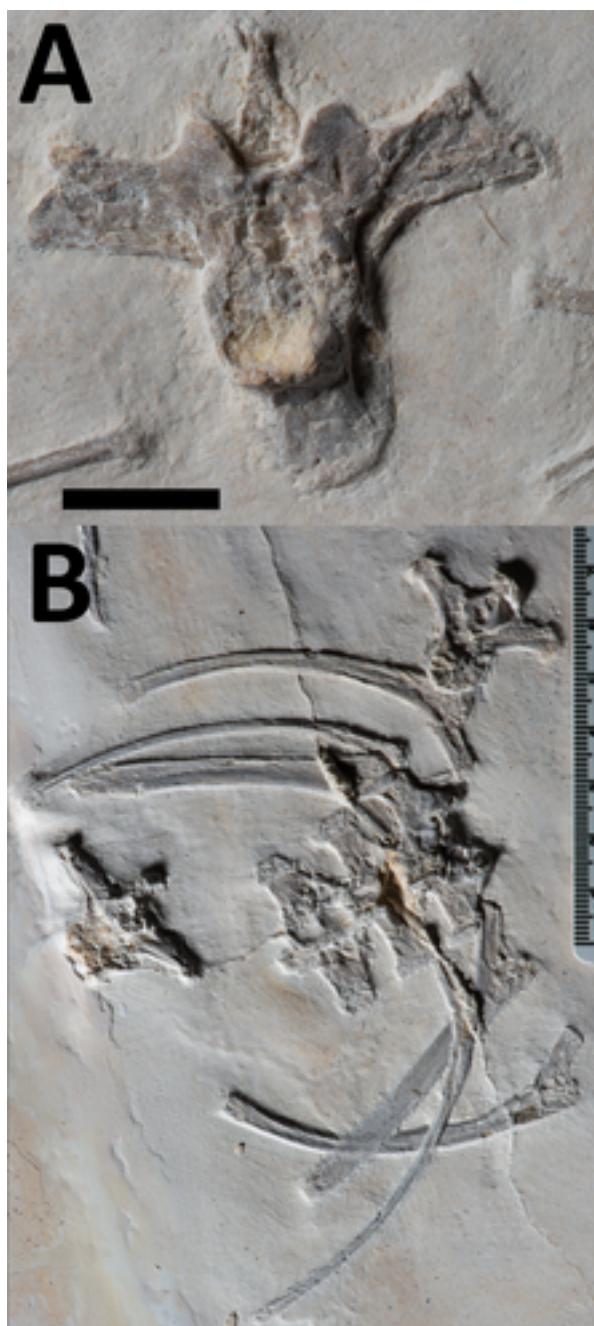


FIGURE 8. Close up of dorsal vertebrae of *Petrodactyle*. A, single mid dorsal seen in posteroventral view (scale bar is 10 mm), and B, anterior dorsal vertebral series seen in dorsal view with articulated anterior dorsal ribs, and two disarticulated dorsal vertebrae seen in anterior view (scale bar with 1 mm divisions).

vertebrae have fused into a notarium as seen in many larger pterodactyloids.

Other axial elements. Several sacral vertebrae are preserved as part of a synsacrum (see following section). No pneumatic openings are visible on any of the vertebrae in the axial column (Figure 9).

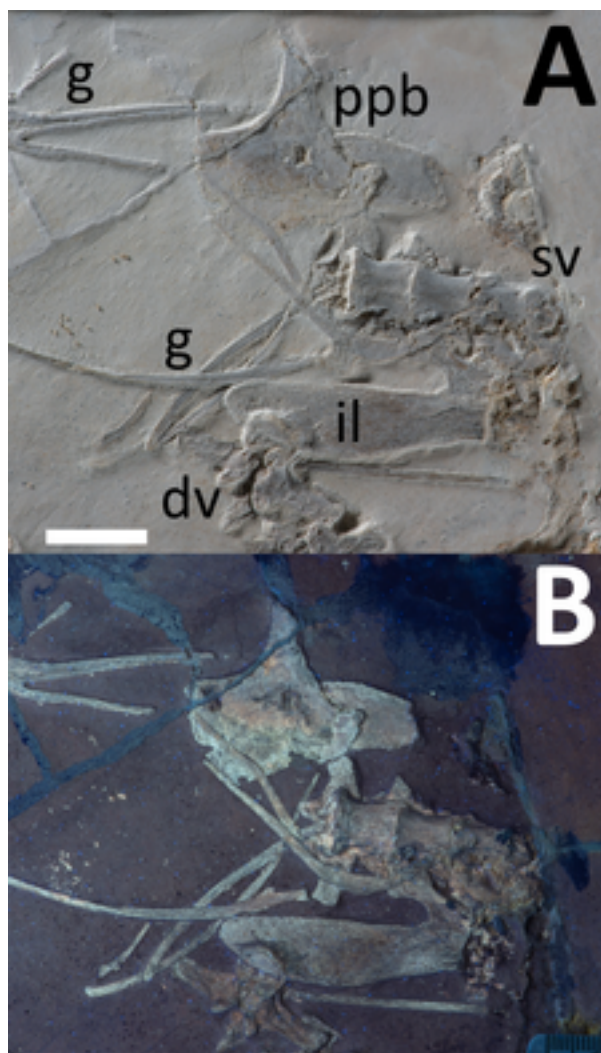


FIGURE 9. Close up of the pelvic region of *Petrodactyle* in A, natural light and B, a mixture of UV AB and C light. Abbreviations are as in Figure 3. Scale bar for both is 20 mm.

A total of 16 dorsal ribs are preserved. These vary in length and curvature but are mostly long, thin, and curved elements. Notably, several of these are especially thickened (more than twice the width of the other ribs) and represent the proximal most pairs of ribs (Figure 8B), as is often seen in ctenochasmatids. These are associated and are in near articulation with the articulated set of anterior dorsal vertebrae.

Four gastralia are preserved in two pairs, suggesting a certain degree of articulation. These are V-shaped with a very wide angle and in two of them, a pronounced thickening in the middle part.

There is a single sternal rib (intercostal rib) preserved. This is a short and simple boomerang-shaped element with one ramus being shorter with

a square end and the other long and tapering to a point.

Girdles. One scapulocoracoid is preserved as an indistinct mass of bone close to the humerus and part of both wings (Figure 10). Although it is very indistinct, it is a large and C-shaped piece of bone with a clearly preserved medial margin showing its outline. A second indistinct patch of bone close to it likely represents the second scapulocoracoid, though this is uncertain. The sternum is not preserved.

Only part of the pelvis is preserved (Figure 9). There is a series of four anterior vertebrae preserved and fused together seen in ventral view. The first of these has laterally projecting processes that do not reach the iliac wings, and thus this is considered a scaralised dorsal that forms part of a synsacrum. There is a partially visible suture between this vertebra and the successive sacral vertebrae. The successive vertebrae are smaller in size and with posteriorly projecting sacral ribs that are fully fused to the ilia and so are true sacral vertebrae. The anterior parts of the ilia are preserved with the two anteriorly projecting wings seen in what is likely lateral view, but they have rotated under crushing and so lie parallel to the synsacrum. They are long and rounded and are broadest at the midpoint. The rest of the pelvis is not preserved.

One of the two prepubes is present and well-preserved (Figure 9). As with many other pterodactyloids it is roughly semicircular in shape with a single projection from the midpart of the straight edge. This is surprisingly thin and both the shape, and even the texture, of the underlying anterior ramus of the ilium is visible through the prepubis.

Forelimbs. Both forelimbs are nearly complete, with only one humerus, a radius and ulna, and some manual phalanges of digits 1-3 missing (Figures 3, 11, see Table 1 for measurements).

The single humerus is very poorly preserved and present only in outline and some bone shards. It is short and robust, but no other details are visible. It is identified on its size and shape, but it does also lie close to the scapulocoracoids and the radius and ulna and other wing elements. It is possible that the second humerus is present as part of the large mass here identified as the scapulocoracoids, or as part of the large indistinct mass lying between these and the partial pelvis, but this is very difficult to determine.

A radius and ulna are preserved lying parallel to one another, but slightly separated. For both elements, both ends are missing, and these are poorly

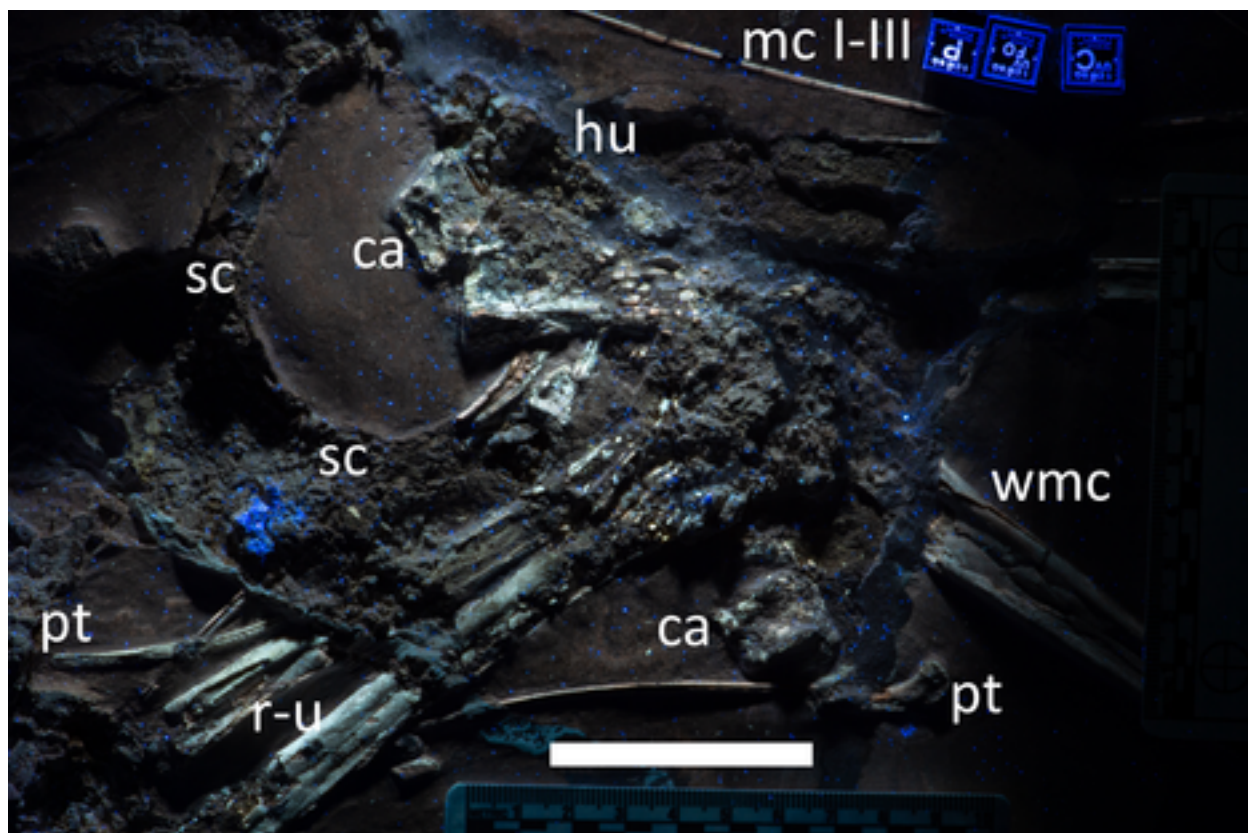


FIGURE 10. Close up of the poorly preserved area of the *Petrodactyle* holotype that contains the pectoral girdles, seen under UV C light to highlight the bone fragments. Abbreviations as in Figure 3. Scale bar is 50 mm.

preserved, so it cannot be determined which element is which. Both are long and straight and are subequal in length and width.

There are several carpals preserved of varying quality (Figures 10, 11). All are roughly square elements and so represent the typically osteologically mature pterosaurian form of a single proximal and distal syncarpal in each wing. The best preserved of these elements is considered here to be a proximal carpal seen in proximal view.

One pteroid is preserved and a second is likely present, but largely hidden by the radius/ulna and a poorly preserved region of bone (Figures 10, 11). The well-preserved pteroid has a pair of small breaks in it, but is otherwise complete, though the very tip may also be covered by the radius or ulna. It is L-shaped with the head offset at a sharp angle to the main body, long (at least 104 mm) and thin, with a concave curvature to the shaft.

Metacarpals I-III are preserved and near complete for both wings (Figure 11). Unusually for pterosaurs, these have disarticulated and are free of the two wing metacarpals. These are subequal in length to that of the wing metacarpal, MC I has an expanded proximal end but those of II and III

taper to a point. All have expanded distal ends and of these, MC I has the most robust expansion. Both wing metacarpals are preserved, although one has part of the shaft missing and the other has its proximal end missing (Figure 4). In both cases, the missing parts are partially represented by poorly preserved bone. These are preserved in medial view showing the expanded distal condyles that are typical for pterosaurs.

Four, and possibly five, phalanges of digits I-III are preserved close to the two sets of metacarpals I-III (Figure 11). These are robust and tapering elements with strongly ginglymoid ends, and likely represent proximal phalanges from the free fingers. No manual unguals are preserved.

The first wing phalanx is large and straight and with a typically 'hooked' proximal end with the full fusion of the extensor tendon process onto the anterior margin of each respective element. The other three distal wing phalanges are all straight elements (notably including the fourth, which is often posteriorly curved in pterosaurs). They taper along their lengths so in addition to each element being shorter than the preceding one, they are also noticeably thinner.



FIGURE 11. Close up of manual elements of *Petrodactyle*. In a mixture of UV A, B and C light. Abbreviations as in Figure 3. Scale bar is 100 mm.

Hindlimbs. The right femur is present in posterior view, but poorly preserved and only the distal part of the shaft and articular end is present, with the rest left as an indistinct outline with some limited bone shards (Figure 3). The distal end is robust with a broad condyle.

A single tibia and fibula and parts of one pes are preserved. Based on the presence of the right femur these are inferred to also be part of the right leg, but this cannot be confirmed.

The tibia is a long and straight element that is preserved in lateral view as seen by the distinctly

expanded and near circular distal condyle. The head of the fibula is present and appressed to the tibia - unlike the rest of the skeleton this has not dissociated suggesting that it may have been fused to the tibia, though this does not appear to be the case. Only the proximal part of the fibula shaft is visible, and it lies partly under one of the cervical vertebrae. It does not appear from the other side, so it is not clear if the element was short, partly broken, fused to the tibia, or is hidden under the tibia further down. The shaft is very narrow, approximately one quarter of the diameter of the tibia at the point that it is no longer visible.

One small and nearly circular-shaped bone is preserved close to the pteroid and is likely to be a distal tarsal or a sesamoid. A second small element lying close to the cervical vertebrae may also be an ankle element, though it is also perhaps a small manual phalanx. Parts of what is likely to be a single pes are preserved. There are a series of three metatarsals preserved together in near articulation and a fourth lying close by, the two largest of these are nearly 50 mm in length. These are long, straight, and simple elements with very little expansion at either end (Figure 3). One of the fifth metatarsals is present as a comma-shaped bone lying close to the posterior part of the skull (Figure 5). At least seven pedal phalanges are preserved in addition to two pedal unguals. These are diagnosed based on their size (they are considerably smaller than the manual phalanges) and location (most lie close to the other hindlimb elements). Most of the preserved pedal elements are long and only one of the very short phalanges of the pes is preserved. The two unguals are short and deep with limited curvature.

Soft tissues and features under UV light. The specimen was photographically documented under visible light and also ultraviolet light (UV A, B, and C wavelengths used individually and/or all together at once), further evaluations were made with the use of a UV flashlight directed at an oblique angle to identify topographical structures. Fluorescent mineralization(s) (if present in the specimen) provide the ability to discern fine structures of bones, skin and teeth, trace structures, and surface treatments that are not normally identified in visible light alone. Under direct application of ultraviolet light wavelengths, the specimen and matrix fluoresced with distinctly different responses (Ultraviolet Induced Fluorescence – UVIF), the fluorescent response was observed in the visible light spectrum, photographed, and analyzed. Although there are no obvious traces of preserved soft tissues on

TABLE 1. List of measurements (top) and proportions (below) of *Petrodactyle* and other large Late Jurassic ctenochasmatids. All measurements are to the nearest mm. The table of measurements data forms the basis of the Nopsca curves in Figure 12.

Taxon	Specimen	Source	Skull	Humerus	Radius /					Femur	Tibia	
					Ulna	WMC	WPX 1	WPX 2	WPX 3			WPX 4
<i>Petrodactyle</i>	LF 2809	Specimen	258	92	x	198	246	176	121	105	134	229
<i>Ctenochasma</i>	BSP 1935.I.24	Bennett, 2007	104	38.5	52.5	52	66	57	x	x	35	55
<i>Gallodactylus</i>	MNHN CNJ71	Bennett, 2013b	x	x	x	x	x	132	94.3	x	101.5	144
<i>Cycnorhamphus</i>	GPIT 80	Bennett, 2013b	160	64	88	111	142	117	85	71	77.5	121
<i>Ardeadactylus</i>	SMNS 56603	Wellnhofer, 1970	215	78	104	130	160	109	77.5	65	99	149
<i>Auroroazhdarcho</i>	NMB Sh 110	Elgin and Hone, 2020	x	63	84	99	123	85	59	52	79	116
<i>Balaeonognathus</i>	NKMB P2011-633	Martill et al., 2023	168	66	87	99	132	99	77	63	71	114

Taxon	Skull / Humerus	Humerus / WMC	WMC / WPX 1	WPX 1 / 2	WPX 2 / 3	WPX 3 / 4	Humerus / Femur	Femur / Tibia
<i>Petrodactyle</i>	2.8	0.5	0.8	1.4	1.5	1.2	0.7	0.6
<i>Ctenochasma</i>	2.7	0.7	0.8	1.2	x	x	1.1	0.6
<i>Gallodactylus</i>	x	x	x	x	1.4	x	x	0.7
<i>Cycnorhamphus</i>	2.5	0.6	0.8	1.2	1.4	1.2	0.8	0.6
<i>Ardeadactylus</i>	2.8	0.6	0.8	1.5	1.4	1.2	0.8	0.7
<i>Auroroazhdarcho</i>	x	0.6	0.8	1.4	1.4	1.1	0.8	0.7
<i>Balaeonognathus</i>	2.5	0.7	0.8	1.3	1.3	1.2	0.9	0.6

the specimen, there are impressions of fine structures which were identified with the use of ultraviolet illumination.

Petrodactyle was found in the Schaudiberg Quarry near Muhlheim, Bavaria, Germany, in the Dritte Rosa Layer (Third Pink layer) of the Mornshheim Formation. As the name of this deposit layer suggests, the mineralisations of this layer have a somewhat pink to orange underlying coloration rather than the more commonly known off-white to yellow “jura” coloured layers from most Solnhofen archipelago deposits. These somewhat pink to orange toned mineralisations are also seen within the bones, claws, and teeth of *Petrodactyle*. The bones and claws are generally identified with an off-white to slightly pink-orange fluorescent colour, and the teeth fluoresce with a vibrant orange tone on the enamel portion of the teeth.

The types and purity of mineralisations within this slab varies across this matrix, which impact the fossil preservation quality, colour, and texture of bones, teeth, and other elements. While most of

the bones were generally well preserved, the upper right corner of the matrix (as orientated in e.g., Figures 1, 2) reveals a very different mineralisation. This localized section of the matrix is dark orange-brown to rusty colour and has a very different texture than the rest of the matrix. The bones within this area are less well preserved, some are poorly discernable, and some cannot be discerned at all. The colour of this material suggests iron mineralisation, and it appears to have more clay content. This is positioned lower than the rest of the matrix in the slab in something of a depression. This iron mineralization is clearly seen under ultraviolet light, which poorly fluoresces if at all, and this is also consistent with areas known to contain iron mineralisations. In addition, rings of similarly coloured mineralisations are seen on the surface of the full matrix with ultraviolet light.

The skull shows a somewhat greenish fluorescent coloration over most of the element (Figure 4), this could be due to mineralisation, but it is more likely due to the application of a consolidant or var-

nish surface treatment to stabilise the bone. While this fluorescent colour is somewhat less common than is normally observed in lithographic limestone fossils from the Solnhofen archipelago, it is interpreted to be the ultraviolet fluorescence induced response of the surface treatment material against the underlying yellow "jura" with pink-orange coloured mineralisation of the deposit layer of the specimen, which resulted in the dull greenish-blue fluorescent colour seen here. This interpretation is reinforced by the observation of some sections of the skull elements which appear to be somewhat crushed and/or contain fragile bone material such as the anterior tips of the mandibles, except at the midline where the lower jaws meet (Figure 4B), and some sections of the lower jaw. The anterior part of the skull also fluoresced with a somewhat greenish-blue colouration under ultraviolet light (Figure 6B), which would likely have been treated with a surface treatment to protect these structures. These are in fact the same areas of the skull which are noted with the dull greenish-blue colouration.

However, more solid sections of bone, such as structures on the posterior portion of the skull are darker, but consistent with the pink-orange tone as seen on all other bones such as the posterior mandible elements, the area where the mandibles join in the center of the lower jaw, and all other limb, wing, and torso bones are presented in an off-white to somewhat pink-orange coloured fluorescence (Figure 4). These fluorescent colours may vary slightly depending upon the localized mineralisation and the use of surface treatments as explained earlier within this deposit (e.g., Figures 9, 11). This UVIF response is commonly seen in species from the Solnhofen archipelago, including pterosaurs, as is also seen in the Painten 'propterodactyloid' under UV light (Tischlinger and Frey, 2013).

In contrast, some thinner and more fragile bone elements (either split, crushed, or very thin) are somewhat translucent under ultraviolet light, which permits the light to penetrate through the bone and results in a somewhat different fluorescent UVIF colouration. Less commonly, a bright pink fluorescence is seen, particularly on delicate wing and limb bones of pterosaurs. In areas where these bones are broken or split, the ultraviolet light may penetrate through the bone and react with underlying matrix and/or stone set material, resulting in this fluorescent response in lithographic limestone fossils from the Solnhofen area (RL pers. obs.).

The dentition of the upper jaw around the teeth and the mid-section of the lower dentaries fluoresced as patches of blue to purple (Figure 4B), suggesting glue was applied. Obliquely angled raked UV light revealed slight impressions of trace structures in the matrix of forward projecting anterior teeth which have been displaced.

The outer edge of the upper rostrum and the outer edges of the lower jaw mid-shaft displayed a gold to brownish colored fluorescence under UV, this was distinctly different from all other areas in this specimen, and a nondescript slightly rectangular pattern is seen with obliquely angled UV light, but it cannot be determined with certainty if these areas are evidence of soft tissue preservation or are bone.

On the anterior dorsal rostrum above the dentition area a low, and uniform bony structure is seen with vertically oriented striations, which fluoresced under UVIF in a gold to brownish coloration. These structures are also seen on the posterior portion of the skull with the same coloration, and vertically orientated striations but are greatly reduced in height and trails to its lowest height over the orbit socket. These striations may represent very fine parts of the bony rostral crest.

The anterior portion of the rostral crest structure fluoresced under UVIF with a light bluish-green fluorescence, likely due to the more delicate, thin, filamentous-like and brittle structures which were most likely treated with some form of consolidant and/or may also contain phosphatic traces. The posterior portion of the crest structure appears to be less delicate and is more uniform in structure, with vertically oriented striations and fluoresced with a pink-orange coloration which is consistent with most other bones seen on the skull. The use of obliquely directed raked UV light revealed fine striated trace impressions in the matrix above the bony crest. These structures are consistent with the structures of the crest, they do not appear to be tool marks, and are interpreted to be a trace structure of the impression of the crest that is not preserved. A slight discoloration and difference in the texture of the matrix above the bony crest is interpreted as potentially a trace impression of poorly preserved soft tissues.

There also are some very fine striations on the matrix close to the displaced palate and inside the NAOF. These trace structures are far too fine to be preparation marks and are not seen elsewhere on the surface of the matrix. They show up as textured ridges under oblique light, rather than being fluo-

rescent, and therefore may represent the impression of some kind of trace of soft tissue.

There are patches of green coloured sediments (under UV A, B, and C together) below the middle part of the skull, along the left side of the mandible and medially to the right articular (Figure 4B). These have no clear structure, but their colour does not match the surrounding matrix and similarly coloured patches on the skull and mandible are in line with each other despite being well separated on the slab and suggests a connection between the two. We suggest that these might be traces of soft tissues, which are weakly phosphatised and are somewhat fluorescent as seen on e.g., *Scaphognathus* (Jäger et al., 2018), but it is more likely due to the use of a consolidant or varnish to stabilize the surface as seen on many of the elements of the skull.

Trace materials commonly used during fossil preparation are seen such as in areas where repairs and/or restoration have been made and are seen as dark blue to purple coloured fluorescence and indicate where glue has been applied. However, more diluted applications of glue may appear as a general light blue (similar to the fluorescence of most varnishes, and also phosphatic material). Areas which appear as a black coloration suggests areas which have been painted, and/or areas where resins have been used (e.g., see Figure 9B), as well as areas of heavy metal mineralisations and dendrites. Areas which fluoresce with a pale blue colouration which are not specific to a particular area may be weakly phosphatised, and/or indicate diluted glue residue, adhesive tape residue, or the application of varnish or other surface treatment as are commonly used to stabilize and protect delicate surface structures.

Taxonomic Identity and Comparisons

Clades. *Petrodactyle wellnhoferi* is clearly a member of the Euctenochasmatia based on the presence of a round orbit that is placed high in the skull (Vidovic and Martill, 2018) and a subhorizontal quadrate, and elongate mid series cervical vertebrae that have a depressed neural arch and a low neural spine (Unwin, 2003). Furthermore, it is a member of the Ctenochasmatoidea based on the dorsal and occlusal surfaces of the rostrum being approximately parallel, the teeth not appearing below the antorbital fenestra (Vidovic and Martill, 2018) (Figure 4). The new genus also has a single feature that is unambiguously present that would place it within the Ctenochasmatidae (sensu

Vidovic and Martill, 2018), the anterior position of the fusion of the dentaries.

Within the Ctenochasmatidae, among traits used to define the more restrictive Gallodactylidae by Kellner (2003), *Petrodactyle* lacks the reduced nasal process, but does show the presence of a parietal crest with a rounded margin that projects to the rear of the skull, teeth confined to the anterior margin of the jaws, and combined humerus and ulna lengths being about 80% of the length of the femur and tibia (Table 1). However, for the traits used by Vidovic and Martill (2018) to define this clade, *Petrodactyle* does have splenial shelves, but these are fused to the symphysis unlike other members of this clade, and it lacks the presence of an acute angle on the dorsal process of the jugal.

Petrodactyle does show two traits that would place it within the Aurorazhdarchidae of Vidovic and Martill (2018) in having mesial and distal teeth with similar length to width ratios and the presence of a ventrally directed bony process on the upper jaw. This does not necessarily resolve the issue, however, as the latter trait is one also seen in the gallodactylid *Cycnorhamphus* and, while these typically have a reduced number of teeth, the former trait arguably also applies to this genus.

As such, it is not entirely clear to which subclade of the Ctenochasmatidae that *Petrodactyle* may belong. It clearly is a derived ctenochasmatid with affinities for more than one clade depending on the characters being used to define these and their exact content. We consider *Petrodactyle* to be probably closest to the Gallodactylidae, though possibly sitting outside this clade as its nearest relative. We note that multiple different recent phylogenies that included numerous ctenochasmatids (e.g., Martill et al., 2023; Yu et al., 2023) have all recovered different arrangements of various genera and there is no clear and unified phylogeny for these taxa. As such, the placement of *Petrodactyle* into one subclade or another is likely cryptic in part because it is not clear how these should be defined, or which other taxa belong there.

Taxonomic comparisons. *Petrodactyle* is a large animal, and it is possible that it is an exceptional morph of another known taxon only with unusual features and proportions because of its size. Although some pterosaurs have been shown to be remarkably isometric in their growth (e.g., Hone et al., 2020), this pattern is probably not universal and there will be intraspecific variation. Thus, although various proportions of elements and series (e.g., the length of the wing finger) of pterosaurs have been repeatedly, and often correctly, used to diag-

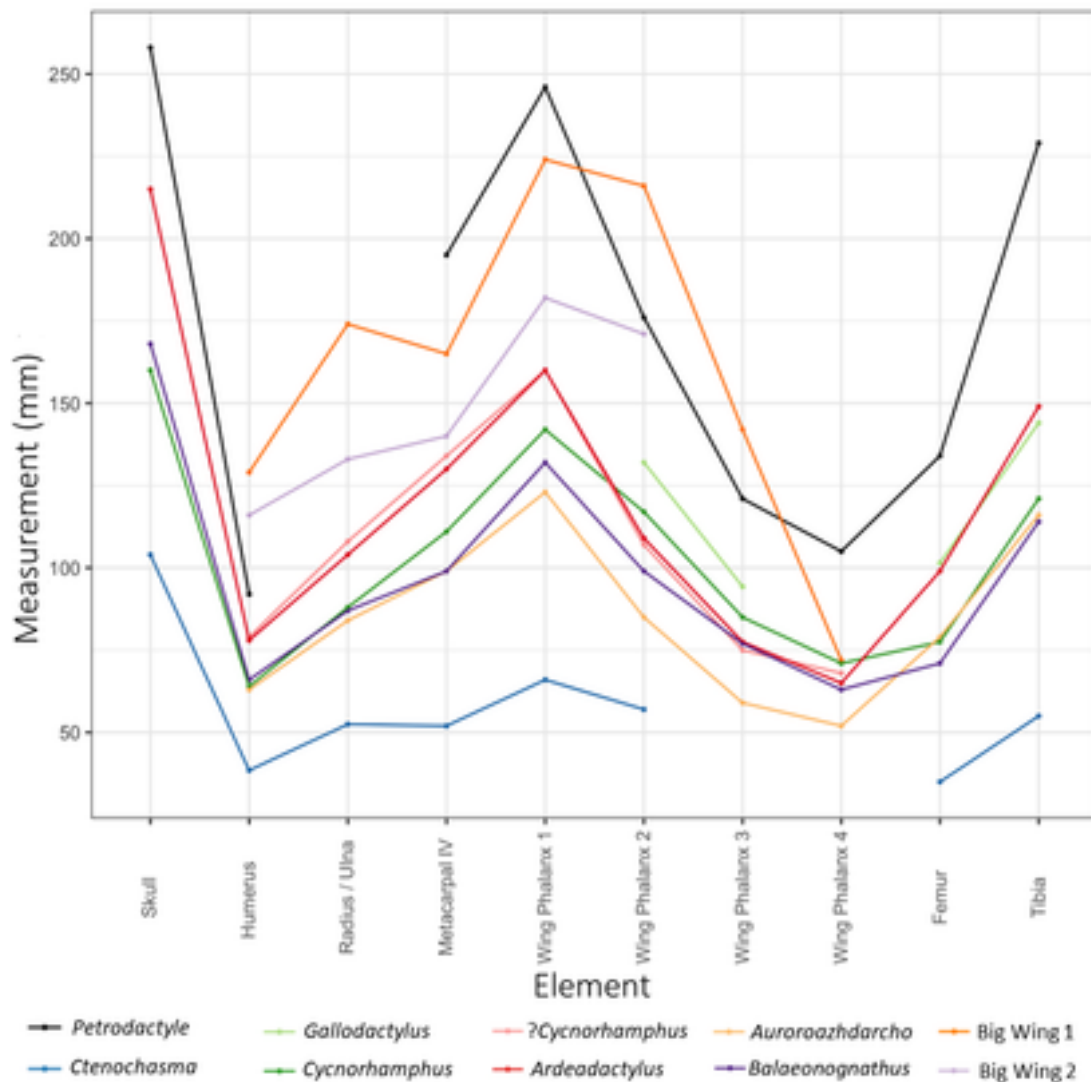


FIGURE 12. ‘Nopsca chart’ showing major proportions of the skeleton comparing *Petrodactyle* to other large Solnhofen region ctenochasmatids (data in Table 1). *Petrodactyle* shows a similar pattern to other animals, though with a proportionally larger head and a long tibia.

nose clades, genera, and species, ontogenetic changes and intraspecific variation should not be overlooked. For example, measurements taken by Bennett (2013b) of two specimens of *Cycnorhamphus* that differ in size by only approximately 30% in humeral size show differences in ratios between various wing and limb elements varying from 1.11 (wing phalanx 3) to 1.32 (femur). Such data therefore remains important for pterosaur taxonomy, but should not be overly relied upon.

The size of *Petrodactyle* is notable (Table 1) and it is considerably larger than most of the taxa known from the Solnhofen archipelago and associated beds, including those recognised from fully mature specimens. For example, Bennett (1996) gives the upper values for skull lengths of a wide

variety of Bavarian ctenochasmatids with only the largest, *Gnathosaurus* (230–280 mm) being close to the c. 260 mm long skull of *Petrodactyle*. Many other taxa are a fraction of this size, even based on their largest known specimens—*Pterodactylus antiquus* at 140 mm, *Ctenochasma gracile* at 200 mm, and *Germanodactylus cristatus* at 130 mm (all taken from Bennett, 1996, and see Table 2). As such, *Petrodactyle* is immediately well separated from the various small ctenochasmatids such as *Germanodactylus*, *Pterodactylus*, *Diopecephalus*, and *Aerodactylus*. Its morphology and proportions are also different to that of larger ctenochasmatids (Figure 12), and such dramatic differences in proportions emerging late in ontogeny compared to

taxa that are only a little smaller would be unparalleled for pterosaurs.

In addition to the diagnostic traits given above, the following traits can be used to separate *Petrodactyle* clearly from other ctenochasmatid taxa from associated fossiliferous beds in the Solnhofen archipelago. *Petrodactyle* can easily be separated from both *Gnathosaurus* and *Ctenochasma* as it lacks the proximal jaw expansion of the former (Wellnhofer, 1970) and the extreme elongation of the jaws of the latter (Wellnhofer, 1970). *Gnathosaurus* has its teeth angled forwards and has widely spaced teeth at the back of the jaws, and *Ctenochasma* has elongate teeth that are angled forwards and are closely spaced (Bennett, 1996), and neither of these features matches the dentition seen here. Similarly, the recently named *Balaenognathus* (Martill et al., 2023) is clearly distinct from *Petrodactyle* given the expanded jaw tips of the former that contain nearly 500 teeth, and so stands in clear contrast to the condition seen here.

The teeth of *Auroroazhdarcho* are long and curving and spaced close together (Bennett, 2013a) unlike those of *Petrodactyle*. In larger specimens of the former, the ratio of the first and second wing phalanx lengths is as little as 59%, a value that is lower than smaller individuals (Bennett, 2013a), which contrasts with the high value of c. 87% here. Finally, *Auroroazhdarcho* has a straight pteroid (Vidovic and Martill, 2014), unlike the sigmoidal one seen in *Petrodactyle*.

Ardeadactylus shows some similarities to *Petrodactyle*, and both exhibit a number of traits that Bennett (2013a) considered diagnostic for the former. These include the evenly spaced teeth with a tooth row that makes up around 50% of the jaw length, and an upper tooth row that does not extend under the NAOF. However, with 23 teeth in the upper jaw, *Petrodactyle* has considerably more teeth than the typical count of 15 of *Ardeadactylus*. The latter also has anterior and posterior teeth that are similar sizes (Bennett, 2013a), which is not seen in *Petrodactyle*, and the teeth here extend in their spacing along the tooth row and do not remain even throughout (Figure 13). *Petrodactyle* has a ratio of the first and second wing phalanx lengths of c. 87% compared to 65-71% in *Ardeadactylus* (Bennett, 2013a). Finally, the greatly elongate cervical vertebrae that are characteristic of *Ardeadactylus* (Bennett, 2013a) are longer than seen here, and the cervical series of *Petrodactyle* is more varied with several shorter cervicals. Thus, despite some similarities, these two taxa are clearly distinct.

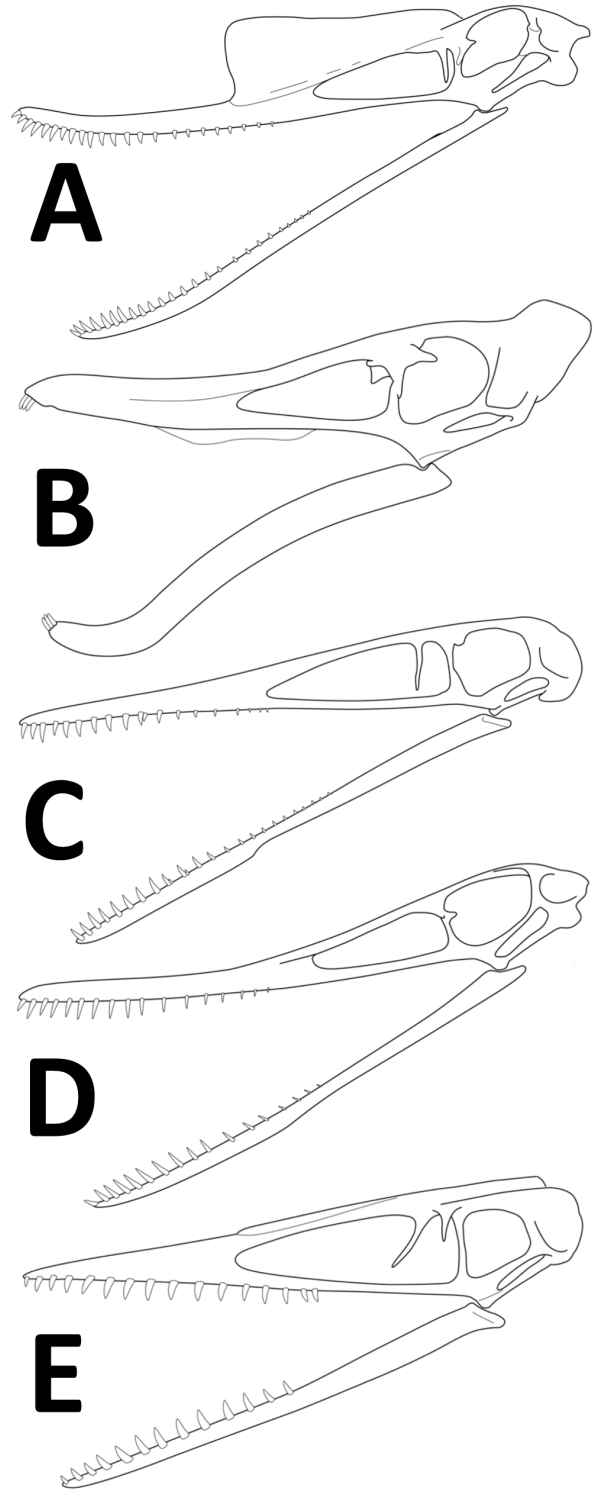


FIGURE 13. Comparison drawing of restored skulls of assorted Solnhofen ctenochasmatids (not to scale). A, *Petrodactyle*; B, *Cycnorhamphus* (following Bennett, 2013); C, *Pterodactylus* (following Wellnhofer, 1970), D, *Ardeadactylus*; E, *Germanodactylus* (following Unwin, 2003).

TABLE 2. List of ctenochasmatoïd pterosaurian taxa from different formations of the Solnhofen region.

Formation	Taxon	Source
Mörnsheim	<i>Pterodactylus antiquus</i>	Barrett et al., 2008
	<i>Diopecephalus kochi</i>	Barrett et al., 2008
	<i>Ardeadactylus longicollum</i>	Barrett et al., 2008
	<i>Germanodactylus cristatus</i>	Bennett, 2007
	<i>Altmuehlopterus rhamphastinus</i>	Barrett et al., 2008
Solnhofen	<i>Cycnorhamphus suevicus</i>	Barrett et al., 2008
	<i>Aerodactylus scolopaciceps</i>	Vidovic and Martill, 2014
	<i>Diopecephalus kochi</i>	Barrett et al., 2008
	<i>Ctenochasma elegans</i>	Barrett et al., 2008
	<i>Gnathosaurus subulatus</i>	Barrett et al., 2008
	<i>Cycnorhamphus suevicus</i>	Barrett et al., 2008
	<i>Auroroazhdarcho primordius</i>	Bennett, 2013b
	<i>Germanodactylus cristatus</i>	Barrett et al., 2008
Painten	<i>Cycnorhamphus suevicus</i>	Bennett, 2013a
	<i>Pterodactylus antiquus</i>	Augustin et al., 2022
Torleite	<i>Balaenognathus maeuseri</i>	Martill et al., 2023

Similarly, there are several key characters in *Cycnorhamphus* that are similar to those present in *Pterodactyle*. Both have a robust skull with a large, striated crest on the rostrum, and a frontoparietal crest at the back of the skull (Figure 13). Both have elongate metacarpals I-III and similar proportions in the wing finger elements, and a long tibia. However, *Cycnorhamphus* has a number of features that clearly separate it from *Pterodactyle*. First, it has teeth limited to the front of the jaws, and a greatly enlarged symphysis to the dentaries (Bennett, 2013b) which are not seen here. *Cycnorhamphus* also has a straight pteroid (Vidovic and Martill, 2018), unlike the curved one seen here. The nasal process in the NAOF is long and ventrally directed in *Pterodactyle* whereas this is reduced in *Cycnorhamphus* (and also *Gallodactylus*, Kellner, 2003). The skull as a whole is shorter and more robust in *Cycnorhamphus*, and the frontoparietal crest is much larger in this taxon than in *Pterodactyle*.

In addition to being considerably larger than adult specimens of the closely related *Pterodactylus*, *Diopecephalus*, and *Aerodactylus*, *Pterodactyle* lacks the greatly elongated and low rostrum of these taxa (Vidovic and Martill, 2014). The spacing of the teeth is also more regular than that of *Aerodactylus*. In *Pterodactylus* the elongate tooth row finishes well under the NAOF (Bennett, 2013a), and the bony crest lacks fine striations as seen here. *Diopecephalus* has a tooth row that contin-

ues under the NAOF (Vidovic and Martill, 2018) which is not seen in *Pterodactyle*. The latter also has cervical vertebrae that are as long as the skull is deep, whereas these are less than 50% of the skull height in *Diopecephalus* (Vidovic and Martill, 2018).

Moving outside of the Solnhofen archipelago the very fragmentary and so far, only known specimen of *Normannognathus* (Buffetaut et al., 1998) has strong similarities with *Pterodactyle*. This animal is known only from the anterior part of a snout of the cranium and mandible and shows a long rostrum and a very large anteriorly directed cranial crest that begins anterior to the nasoantorbital fenestra. *Normannognathus* preserves 14 teeth from the point at which the crest begins to the broken jaw tip, of which five are from the premaxilla. However, *Pterodactyle* preserves at least 20 teeth anterior to the crest in the upper jaw, and these vary in size with posterior teeth being markedly smaller than the anterior ones, whereas the alveoli are all of similar sizes in *Normannognathus* (Witton et al., 2015). The posterior end of the dentary symphysis in *Pterodactyle* is level with the fourteenth tooth of the dentary, but in *Normannognathus*, the end of the symphysis is not visible beyond the fourteenth alveoli, although the preserved end of the bone stops shortly after this point. The single preserved tooth of *Normannognathus* is described as being long and slender and anteriorly directed (Witton et al., 2015), and therefore different to the

rather short and conical, vertically orientated teeth, which are seen here.

Finally, the genera *Germanodactylus* and *Altmuehlopterus* have been recovered in various recent analyses as both ctenochasmatids and as basal dsungaripterids (as well as in other clades e.g., Vidovic and Martill, 2018 and Yu et al., 2023) and the exact placement of these remains uncertain. However, both are clearly distinct from *Petrodactyle*, which has far more teeth than either *Germanodactylus* (Figure 13) or *Altmuehlopterus*. *Petrodactyle* also lacks the edentulous jaw tips of *Germanodactylus*, and also lacks the distinctive trait of subequal lengths of the second and third wing phalanges of *Altmuehlopterus* (Vidovic and Martill, 2018).

Given the uncertainty of the exact localities of many historically excavated pterosaur specimens from the region, and that some genera are seen in multiple formations (Table 2), comparisons also need to be made to other prospective taxa beyond the Mörnshheim Formation that produced *Petrodactyle*. In this regard, it is possible that *Petrodactyle* is a far more complete specimen of one of the various isolated ‘big wing’ specimens from Solnhofen area limestones (Elgin and Hone, 2020). *Petrodactyle* is among the largest known pterodactyloids from these beds with the length of the skull being similar to other large pterosaurs from the Solnhofen area, although a little smaller than the largest *Ctenochasma* (Bennett, 2013b). It also has wing elements that are as large, or even larger, than the biggest known specimens of both named taxa and the indeterminate specimens assigned to two different morphotypes by Elgin and Hone (2020). However, although in general the lengths and proportions of available wing elements of *Petrodactyle* are a reasonable match for morphotype 1, and less good for morphotype 2 of Elgin and Hone (2020), the wing metacarpal is rather longer than the ulna (although the ends of the radius and ulna are incomplete, this is clearly the case) in *Petrodactyle* than in either of these (Table 1, Figure 12). As such this is not a clear fit for either of the two morphotypes and suggests that these animals are still different to *Petrodactyle* and likely represent other, as yet unnamed, pterodactyloids.

DISCUSSION

Cranial Crests

Numerous different pterosaur lineages are now known to have had some form of cranial crest. These include crests composed solely of soft tis-

ues, combinations of soft tissues and bone, and potentially those made only of bone (Witton, 2013). The striated sagittal crest on the rostrum of *Petrodactyle* is similar to that borne by a number of other ctenochasmatoid taxa (e.g., see Buffetaut et al., 1998; Frey et al., 2003; Bennett, 2013b, Figure 13), and others including non-pterodactyloid monofenestratans (Lü et al., 2011), *Germanodactylus* (Bennett, 2006) and *Hamipterus* (Wang et al., 2014). In at least some cases, these striated crests support preserved soft tissues crests that can be considerably larger than the supporting bony structure (e.g., Frey and Martill, 1998; Bennett, 2013a). The rostral crest of *Petrodactyle* is considerably larger than that seen on any other ctenochasmatoid pterosaur, even accounting for the large size of the holotype (cf. *Cycnorhamphus*, Figure 13B) with the exception of *Normannognathus* (Buffetaut et al., 1998). The size of the crest is in a large part likely due to the large size of the individual and its near-mature status. Sexually selected structures undergo strong positive allometry and so large and old individuals are likely to bear disproportionately large crests compared to animals that are not necessarily much smaller or younger (Hone et al., 2012b).

It is now well established that the wide variety of cranial crests borne by pterosaurian taxa primarily (or exclusively) functioned as a socio-sexual signal (Hone et al., 2012b). Although there is some good evidence for sexual dimorphism in some pterosaurs, with females having smaller (*Pteranodon* – Bennett, 2001), or not (*Darwinopterus* – Lü et al., 2011) crests, exaggerated structures are likely present in males and females for various taxa (e.g., we are yet to find an adult ornithocheirid without a crest of some kind on its rostrum), and there is no particular reason to suggest this specimen is male or female based on the presence of this crest alone.

A number of ctenochasmatids also bear a soft tissue crest at the back of the skull, often termed the occipital cone or lappet (Frey et al., 2003, Bennett, 2013a), which in some may have integrated with the soft tissue crest attached to the top of the rostrum (Frey et al., 2003, though see Bennett, 2013b). However, this seems unlikely in *Petrodactyle* as there is no simple rounded posterior face to the skull as seen in e.g., *Pterodactylus*. Instead, there is a laterally flattened frontoparietal crest at the back of the skull that is similar to that seen in *Cycnorhamphus* and *Gallodactylus* (Bennett, 2013b), though smaller than either. The crest of the latter is somewhat rounded in shape as compared

to the more triangular form seen in *Petrodactyle*. This posterior crest or expansion in *Cycnorhamphus* is present in juveniles that lack a rostral crest, suggesting this is not under socio-sexual selection but instead, is functionally important. We agree with the interpretation of Bennett (2013b) that this structure anchored larger than usual jaw muscles that would have given animals with this type of crest the ability to have a relatively strong bite even at the tips of the jaws and with the potential for large depression of the jaw (see following section).

Ecology

Ctenochasmatoids were primarily carnivorous animals typically taking small prey, frequently as filter feeders (Witton, 2013; Martill et al., 2023), but there is also evidence of some like *Pterodactylus* eating fish (Witton, 2018 – though the specimen in question is now lost), which lack the extremely numerous teeth and laterally expanded jaw tips of filter feeders such as *Gnathosaurus* or *Ctenochasma*. *Petrodactyle* does not have the closely packed, numerous, and elongate teeth of filter feeders, but instead their teeth are widely spaced as well as being short and much fewer in number. This pattern suggests that they did not act as filter feeders. The teeth are near conical in shape with roots that are longer than the crown but are not especially robust and thickened, suggesting it did not feed on particularly hard prey. Similarly, the jaws are long and thin and not overly robust in *Petrodactyle*, and the dentaries lack the large symphysis seen in *Cycnorhamphus* that would strengthen the jaws. That said, as noted above, the expanded frontoparietal crest at the back of the skull does suggest that the jaws give a relatively strong bite (and this may have been further supported by the expansions on the surangulars), even at the jaw tips, and this matches the dentition being limited to the anterior half of the skull. We infer from this that grip was important for *Petrodactyle*, and was potentially a piscivore catching small fish, but also likely cephalopods, small crustaceans, and even hatchling tetrapods.

This interpretation also generally fits two other recent assessments of the diet of larger ctenochasmatids. Bestwick et al. (2018) assessed the available evidence for the diet of various ctenochasmatoids based on a combination of ichnological and morphological data and that of associated specimens (e.g., gut contents). They interpreted early branching ctenochasmatoids as piscivores and carnivores, and more derived ctenochasmatids as piscivores or filter feeders. Hender-

son (2018) similarly assessed the mechanical performance of the skulls of numerous pterosaurs, and while *Petrodactyle* was obviously not included, he did include close relatives and/or taxa with similar skull shapes in *Gnathosaurus*, *Pterodactylus*, *Cycnorhamphus*, and *Altmulopterus rhamphistinus*. Analysis of skull strength shows that those animals with relatively strong and sharp teeth had considerably stronger and more rigid skulls than those with spatulate jaws and filter-feeding teeth, implying they were processing larger and more resistant foods. The steeply angled quadrate and expanded posterior crest would also serve to orientate some of the jaw closing muscles so that they are closer to right angles to the jaw and allow for a greater application of torque when closing the jaws, giving it a strong bite (Henderson, 2018). The teeth being limited to the front part of the jaws in *Petrodactyle* matches the pattern seen in *Cycnorhamphus* and *Istiodactylus*, which show similar adaptations to strong skulls and powerful bites (Henderson, 2018). Such a behaviour is perhaps also supported by the wear seen here on the tips of the teeth which suggests they were being used on relatively hard prey items such as crustaceans.

The limb proportions of *Petrodactyle* are similar to other large ctenochasmatids (Figure 12) suggesting that they had fundamentally similar flight profiles and terrestrial capabilities. As ctenochasmatids are often considered to be animals that were waders or foraged along shorelines (Witton, 2013) then the length of the legs and size of the feet may be important for wading and support on soft substrates. The tibia is long here, around 1.7 times the length of the femur and the highest proportion recorded for Solnhofen area ctenochasmatoids. The pes in *Petrodactyle* is incomplete, however, metatarsals I-IV are complete, and their lengths can be compared to that of the tibia to see if they are in proportion with other large ctenochasmatids. In *Cycnorhamphus* these vary from 18-21% of the tibial length, in *Gallodactylus* 20-25%, (both Bennett, 2013b), in *Auroroazhdarcho* 15-18% (Frey et al., 2011), and here in *Petrodactyle* this is 19-21% and so is similar.

Petrodactyle would have been terrestrially competent and had the potential to be a wader given its long legs (Figure 14). It would have had a relatively strong skull and powerful bite and is here interpreted as a carnivore, likely feeding predominantly on fish and other accessible prey (and potentially scavenging) in a coastal setting. The Mörnsheim Formation includes appropriate possible prey species in this regard as, for example,

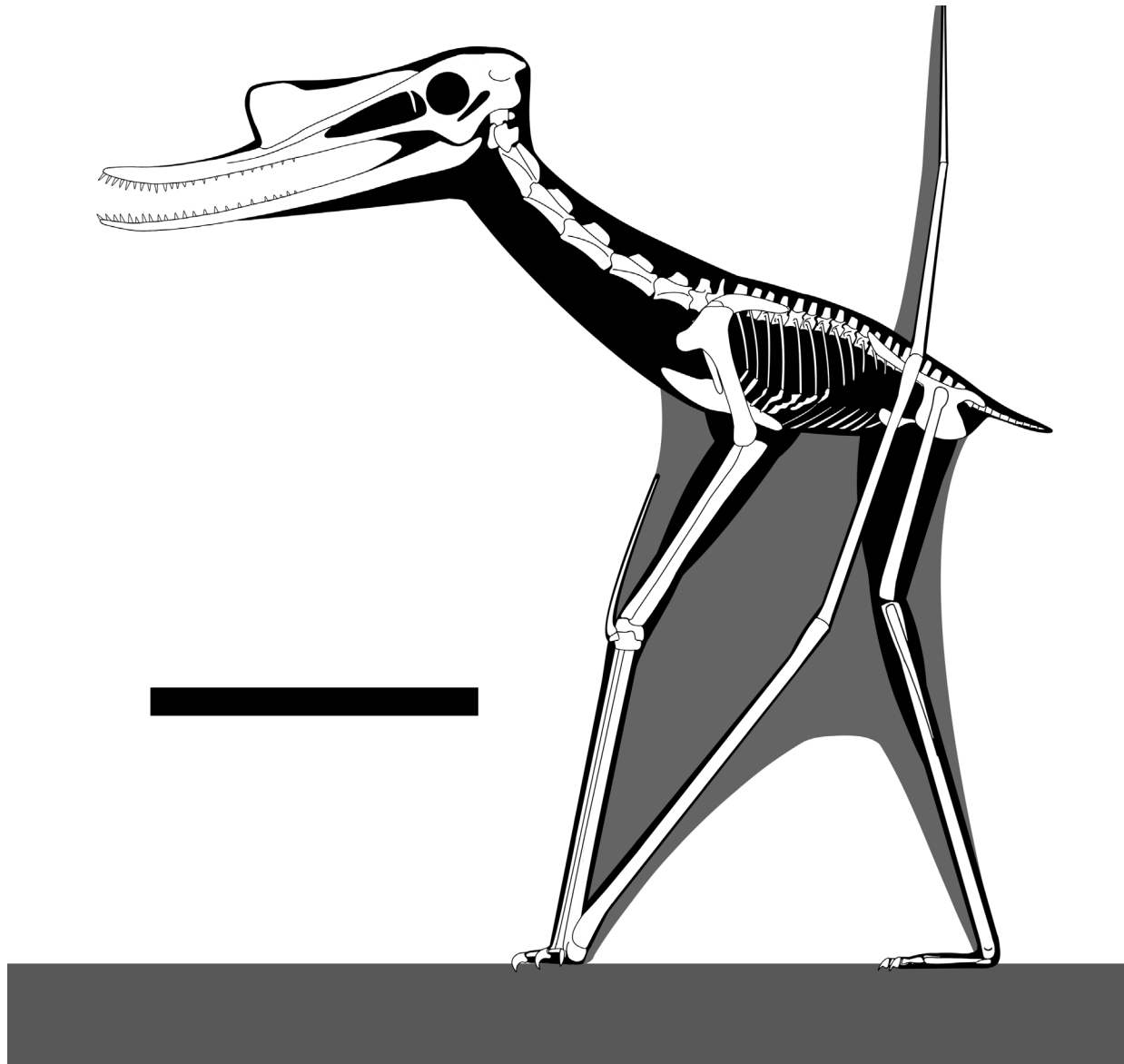


FIGURE 14. Reconstruction of the complete skeleton of *Petrodactyle wellnhoferi* in a standing pose. Scale bar is 200 mm. Missing parts based on *Cycnorhamphus* following Witton (2013).

small teleost fish, shrimp, larvae of slipper lobsters, and small ammonites are all known (Röper, 2005).

Taphonomy

Specimen LF 2809 is almost entirely disarticulated, although many elements remain close to their anatomical neighbours and the specimen is mostly complete (Figure 1). This combination is unusual, and the condition seen here lies in strong contrast with more typical conditions of pterosaur specimens from the Solnhofen archipelago. These either tend to be close to complete and fully articulated, or show evidence of progressive decay with

loss of elements, especially the limbs and skull, as a result of the carcass hanging in the water column (Beardmore et al., 2017).

Here though, nearly all the elements are present. It would not have been hanging in the water column for an extended period and losing elements like teeth, ribs, and manual phalanges without also losing parts such as the skull or the wings as a whole. Although mostly disarticulated, there is also no strong evidence of a current that disturbed the specimen and aligned the long bones (as in e.g., *Gallodactylus*, Fabre, 1976) and the apparent staining of some soft tissues leaching from the

body also support a lack of strong currents. The mandible lies next to the skull and the long bones (especially those of the wing elements) are not all aligned as would be expected from being moved by a current, but instead several are at right angles to each other. Although some have been lost, many small and light elements (e.g., some isolated teeth, metacarpals I-III, manual and pedal elements, gastralia, and ribs) are both present and lying close to their original positions. This suggests therefore that the body sank relatively quickly after death and landed in the sediment intact, but also subsequently underwent substantial decay in order to separate and disarticulate the various skeletal elements. The separation of the radius and ulna is unusual, as is the separation of metacarpals I-III, the separation of the wing finger phalanges from each other, and the loss of some teeth.

Our interpretation of this is therefore that the specimen must have remained exposed on the sea bed for a considerable period prior to burial for this separation to have occurred. The specimen also does not appear to have been accessed by large scavengers which would have caused greater disarticulation, loss, or destruction of elements. There is therefore apparent *in situ* decay, but with only limited or no access by macroscopic carnivores, and with only a limited or no current, hence the limited dispersal of the separated elements.

The specimen was at some point disturbed sufficiently to remove some small elements (manual and pedal phalanges, and ribs) and to move many others (lost teeth, separated out the metacarpals, separated the cervical and dorsal vertebrae). We further suggest that such an event (e.g., a storm or unusually high tide) might have brought in the sediment to finally bury the specimen preventing further decay. The Solnohfen archipelago at this time likely encountered seasonal monsoonal storms (see Bennett, 1996a), which might have caused such an event.

Röper (2005) illustrated the Mörsheim is part of a reef deposit (his figure 10), although Rauhut et al. (2019) consider the Mühlheim locality to be within a basin deposit, though notably very close to ancient sponge reefs. This may support our interpretation with the suggestion of a generally calm region (a basin sheltered by a reef) with occasional breaching or over topping, causing the shift in elements and burial.

This pattern is unusual, though not unique for larger pterodactyloids in this region. The disruption seen to *Petrodactyle* is very similar to the holotype specimen of *Cycnorhamphus* from Painten (Ben-

net, 2013b) which is similarly complete and all joints separated, but there is less spread of the elements here, and also similar to the holotype of *Ardeadactylus* from Nusplingen (Bennett, 2013a). Although large and isolated pterodactyloid wings are known from the area (e.g., Elgin and Hone, 2020) showing that larger specimens do still shed their wings as units, it is notable that there are several larger specimens that are mostly complete but disarticulated across multiple sites and suggests that they may be undergoing a different taphonomic process to smaller animals.

It is not only pterosaurs that may respond this way. The early bird *Alcmonavis* (Rauhut et al., 2019) from the Mörsheim while far less complete is similarly preserved in that the specimen (while only representing one wing) has all the major elements preserved which are associated, but disarticulated, and its elements are preserved nearby and not lost. In short, it is good match for the pattern described here for *Petrodactyle* and suggests some similarities in preservation.

SUMMARY

Although the distribution of pterosaur fossils is rather clumped with a handful of regions producing most of the well-preserved specimens, the discovery of *Petrodactyle* demonstrated that even major formations that have been well studied and excavated over a considerable period continue to produce important new specimens. Ecosystems are often dominated by a small number of species that are represented by numerous individuals and make up much of the biomass, and so it is inevitable that many taxa will be rare and hard to find. Thus, ongoing excavations will be necessary to provide more thorough pictures of the diversity and disparity of lineages such as pterosaurs and to build a more complete picture of their history. In this context, *Petrodactyle wellnhoferi* (Figure 14) is another step closer to a fuller understanding of these flying reptiles.

ACKNOWLEDGEMENTS

We wish to thank two anonymous referees and the editor N. Nasser for their comments, which helped improve an earlier version of this manuscript. DWEH and FS thank the Lauer Foundation for their support. We thank S. McDavid for the reconstruction of the skeleton used in Figure 14. We also thank R. Pöschl and U. Leonhardt for excavating this specimen, and we thank U. Leonhardt for preparation of the specimen and it's docu-

mentation, as well as detailed documentation of the specimen's precise stratigraphy and position in the quarry.

REFERENCES

- Augustin, F.J., Kampouridis, P., Hartung, J., Albersdörfer, R., and Matzke, A.T. 2022. The geologically oldest specimen of *Pterodactylus*: a new exquisitely preserved skeleton from the Upper Jurassic (Kimmeridgian) Plattenkalk deposits of Painten (Bavaria, Germany). *Fossil Record*, 25:331–343.
<https://doi.org/10.3897/fr.25.90692>
- Barrett, P.M., Butler, R.J., Edwards, N.P., and Milner, A.R. 2008. Pterosaur distribution in time and space: an atlas. *Zitteliana*, 28:61–107.
- Beardmore, S.R., Lawlor, E., and Hone, D.W.E. 2017. The taphonomy of Solnhofen pterosaurs reveals soft-tissue anatomical differences between basal and derived forms. *Naturwissenschaften*, 107:1–11.
<https://doi.org/10.1007/s00114-017-1486-0>
- Bennett, S.C. 1995. A statistical study of *Rhamphorhynchus* from the Solnhofen Limestone of Germany: year-classes of a single large species. *Journal of Paleontology*, 69:569–580.
<https://doi.org/10.1017/S0022336000034946>
- Bennett, S.C. 1996. Year-classes of pterosaurs from the Solnhofen Limestone of Germany: taxonomic and systematic implications. *Journal of Vertebrate Paleontology*, 16:432–444.
<https://doi.org/10.1080/02724634.1996.10011332>
- Bennett, S.C. 2001. The osteology and functional morphology of the Late Cretaceous pterosaur *Pteranodon* Part I. General description of osteology. *Palaeontographica Abteilung A*, 260:1–112.
<https://doi.org/10.1127/pala/260/2001/1>
- Bennett, S.C. 2006. Juvenile specimens of the pterosaur *Germanodactylus cristatus*, with a review of the genus. *Journal of Vertebrate Paleontology*, 26:872–878.
[https://doi.org/10.1671/0272-4634\(2006\)26\[872:JSOTPG\]2.0.CO;2](https://doi.org/10.1671/0272-4634(2006)26[872:JSOTPG]2.0.CO;2)
- Bennett, S.C. 2013a. New information on body size and cranial display structures of *Pterodactylus antiquus*, with a revision of the genus. *Paläontologische Zeitschrift*. 2:269–289.
<https://doi.org/10.1007/s12542-012-0159-8>
- Bennett, S.C. 2013b. The morphology and taxonomy of the pterosaur *Cycnorhamphus*. *Neues Jahrbuch für Geologie und Palaeontologie, Abhandlungen*, 267:23–41.
<https://doi.org/10.1127/0077-7749/2012/0295>
- Bestwick, J., Unwin, D.M., Butler, R.J., Henderson, D.M., and Purnell, M.A. 2018. Pterosaur dietary hypotheses: a review of ideas and approaches. *Biological Reviews*, 93:2021–2048.
<https://doi.org/10.1111/brv.12431>
- Buffetaut, E., Lepage, J.-J., and Lepage, G. 1998. A new pterodactyloid pterosaur from the Kimmeridgian of the Cap de la Hève (Normandy, France). *Geological Magazine*, 135:719–722.
<https://doi.org/10.1017/S0016756898001575>
- Cuvier, G. 1809. Mémoire sur le squelette fossile d'un reptile volant des environs d'Aichstedt, que quelques naturalistes ont pris pour un oiseau, et dont nous formons un genre de Sauriens, sous le nom de Petro-Dactyle. *Annales du Muséum national d'Histoire Naturelle*, Paris, 13:424–437.
- Elgin, R.A. and Hone, D.W.E. 2020. A review of two large Jurassic pterodactyloid specimens from the Solnhofen of southern Germany. *Palaeontologica Electronica*, 23:a13.
<https://doi.org/10.26879/741>
- Fabre, J. 1976. Un nouveau Pterodactylidae sur le gisement "Portlandian" de Canjurs (Var): *Gallodactylus canjuersensis* nov. gen., nov. sp. *Comptes Rendus de l'Académie des Sciences*, Paris, 279:2011–2014.

- Frey, E. and Martill, D.M. 1998. Soft tissue preservation in a specimen of *Pterodactylus kochi* (Wagner) from the Upper Jurassic of Germany. *Neues Jahrbuch für Geologie und Paläontologie, Abhandlungen*, 210:421–441.
<https://doi.org/10.1127/njgpa/210/1998/421>
- Frey, E., Meyer, C.A., and Tischlinger, H. 2011. The oldest azhdarchoid pterosaur from the Late Jurassic Solnhofen Limestone (early Tithonian) of southern Germany. *Swiss Journal of Geosciences*, 104:35–55.
<https://doi.org/10.1007/s00015-011-0073-1>
- Frey, E., Tischlinger, H., Buchy, M.C., and Martill, D.M. 2003. New specimens of Pterosauria (Reptilia) with soft parts with implications for pterosaurian anatomy and locomotion. Geological Society, London, Special Publications, 217:233–266.
<https://doi.org/10.1144/GSL.SP.2003.217.01.14>
- Henderson, D.M. 2018. Using three-dimensional, digital models of pterosaur skulls for the investigation of their relative bite forces and feeding styles. Geological Society, London, Special Publications, 455:25–44.
<https://doi.org/10.1144/SP455.9>
- Hone, D.W.E. 2012. Pterosaur research: recent advances and a future revolution. *Acta Geologica Sinica*, 86:1366–1376.
<https://doi.org/10.1111/1755-6724.12006>
- Hone, D.W., Habib, M.B., and Lamanna, M.C. 2013. An annotated and illustrated catalogue of Solnhofen (Upper Jurassic, Germany) pterosaur specimens at Carnegie Museum of Natural History. *Annals of Carnegie Museum*, 82:165–191.
<https://doi.org/10.2992/007.082.0203>
- Hone, D.W.E., Naish, D., and Cuthill, I.C. 2012b. Does mutual sexual selection explain the evolution of head crests in pterosaurs and dinosaurs? *Lethaia*, 45:139–156.
<https://doi.org/10.1111/j.1502-3931.2011.00300.x>
- Hone, D.W.E., Tischlinger, H., Frey, E., and Röper, M. 2012a. A new non-pterodactyloid pterosaur from the Late Jurassic of Southern Germany. *PLoS One*, 7:p.e39312.
<https://doi.org/10.1371/journal.pone.0039312>
- Hone, D.W.E., Ratcliffe, J.M., Riskin, D.K., Hemanson, J.W., and Reisz, R.R. 2020. Unique near isometric ontogeny in the pterosaur *Rhamphorhynchus* suggests hatchlings could fly. *Lethaia*, 54:106112.
<https://doi.org/10.1111/let.12391>
- Jäger, K.R., Tischlinger, H., Oleschinski, G., and Sander, P.M. 2018. Goldfuß was right: Soft part preservation in the Late Jurassic pterosaur *Scaphognathus crassirostris* revealed by reflectance transformation imaging (RTI) and UV light and the auspicious beginnings of paleo-art. *Palaeontologia Electronica*, 21:1–20.
<https://doi.org/10.26879/713>
- Jouve, S. 2004. Description of the skull of a *Ctenochasma* (Pterosauria) from the latest Jurassic of eastern France, with a taxonomic revision of European Tithonian Pterodactyloidea. *Journal of Vertebrate Paleontology*, 24:542–554.
[https://doi.org/10.1671/0272-4634\(2004\)024\[0542:DOTSOA\]2.0.CO;2](https://doi.org/10.1671/0272-4634(2004)024[0542:DOTSOA]2.0.CO;2)
- Kaup, J. 1834. Versuch einer Eintheilung der Säugethiere in 6 Stämme und der Amphibien in 6 Ordnungen. *Isis von Oken*. 1834:315.
- Kellner, A.W.A. 2003. Pterosaur phylogeny and comments on the evolutionary history of the group. Geological Society Special Publications, 217:105–137.
<https://doi.org/10.1144/GSL.SP.2003.217.01.10>
- Kellner, A.W. 2015. Comments on Triassic pterosaurs with discussion about ontogeny and description of new taxa. *Anais da Academia Brasileira de Ciências*, 87:669–689.
<https://doi.org/10.1590/0001-3765201520150307>
- Lü, J., Unwin, D.M., Deeming, D.C., Jin, X., Liu, Y., and Ji, Q. 2011. An egg-adult association, gender, and reproduction in pterosaurs. *Science*, 331:321–324.
<https://doi.org/10.1126/science.1197323>
- Martill, D.M., Frey, E., Tischlinger, H., Mäuser, M., Rivera-Sylva, H.E., and Vidovic, S.U. 2023. A new pterodactyloid pterosaur with a unique filter-feeding apparatus from the Late Jurassic of Germany. *PalZ*, 1–42.
<https://doi.org/10.1007/s12542-022-00644-4>

- Ősi, A., Prondvai, E., and Géczy, B. 2010a. The history of Late Jurassic pterosaurs housed in Hungarian collections and the revision of the holotype of *Pterodactylus micronyx* Meyer 1856 (a 'Pester Exemplar'). Geological Society, London, Special Publications, 343:277–286. <https://doi.org/10.1144/sp343.17>
- Ősi, A., Prondvai, E., Frey, E., and Pohl, B. 2010b. New interpretation of the palate of pterosaurs. The Anatomical Record: Advances in Integrative Anatomy and Evolutionary Biology, 293:243–258. <https://doi.org/10.1002/ar.21053>
- Plieninger, F. 1901. Beiträge zur Kenntniss der Flugsaurier. Paläontographica, 48:65-90.
- Rauhut, O.W., Tischlinger, H., and Foth, C. 2019. A non-archaeopterygid avialan theropod from the Late Jurassic of southern Germany. Elife, 8:p.e43789. <https://doi.org/10.7554/eLife.43789>
- Röper, M. 2005. Field trip C: Lithographic limestones and plattenkalk deposits of the Solnhofen and Mörnsheim formations near Eichstätt and Solnhofen. Zitteliana, 26:71–85.
- Tischlinger, H. and Frey, E. 2013. A new pterosaur with mosaic characters of basal and pterodactyloid pterosauria from the Upper Kimmeridgian of Painten (Upper Palatinate, Germany). Archaeopteryx, 31:1–13.
- Unwin, D.M. 2003. On the phylogeny and evolutionary history of pterosaurs. Evolution and Palaeobiology of Pterosaurs. Geological Society Special Publications, 217:139–190. <https://doi.org/10.1144/GSL.SP.2003.217.01.11>
- Vidovic, S.U. and Martill, D.M. 2014. *Pterodactylus scolopaciceps* Meyer, 1860 (Pterosauria, Pterodactyloidea) from the Upper Jurassic of Bavaria, Germany: The problem of cryptic pterosaur taxa in early ontogeny. PLoS ONE, 9:e110646. <https://doi.org/10.1371/journal.pone.0110646>
- Vidovic, S.U. and Martill, D.M. 2018. The taxonomy and phylogeny of *Diopcephalus kochi* (Wagner, 1837) and '*Germanodactylus rhamphastinus*' (Wagner, 1851). Geological Society, London, Special Publications, 455:125–147. <https://doi.org/10.1144/SP455.12>
- Vullo, R., Heil, J.F., and Dunand, M. 2012, January. On a 19th Century *Pterodactylus* (Pterosauria) specimen held in the Natural History Museum of La Rochelle, France. Annales de Paléontologie, 98:63–69. <https://doi.org/10.1016/j.annpal.2011.11.004>
- Wellnhofer, P. 1970. Die Pterodactyloidea (Pterosauria) der Oberjura-Plattenkalke Süddeutschlands. – Bayerische Akademie der Wissenschaften, Mathematisch-Wissenschaftlichen Klasse, Abhandlungen, 141:1–133
- Wellnhofer, P. 1975. Die Rhamphorhynchoidea (Pterosauria) der Oberjura-Plattenkalke Süddeutschlands. Palaeontographica, Abt. A, 148:1–13.
- Witton, M.P. 2013. *Pterosaurs*. Princeton University Press, Los Angeles, USA. <https://doi.org/10.1515/9781400847655>
- Witton, M.P. 2018. Pterosaurs in Mesozoic food webs: a review of fossil evidence. Geological Society, London, Special Publications, 455:7–23. <https://doi.org/10.1144/SP455.3>
- Witton, M.P., O'Sullivan, M., and Martill, D.M. 2015. The relationships of *Cuspicephalus scarfi* Martill and Etches, 2013 and *Normannognathus wellnhoferi* Buffetaut et al., 1998 to other monofenestratan pterosaurs. Contributions to Zoology, 84:115–127. <https://doi.org/10.1163/18759866-08402002>
- Woodward, A.S. 1902. On two skulls of Ornithosaurian *Rhamphorhynchus*. Annual Magazine of Natural History 9:1. <https://doi.org/10.1080/00222930208678529>
- Yu, Y., Zhang, C., and Xu, X. 2023. Complex macroevolution of pterosaurs. Current Biology, 33:770-779. <https://doi.org/10.1016/j.cub.2023.01.007>